Gas in Scattering Media Absorption Spectroscopy in Large Geometries

- Towards Monitoring Oxygen in Adult Lungs -

LUND UNIVERSITY

Anna Brandt

THESIS PROJECT

Division of Combustion Physics, Department of Physics
Faculty of Engineering, Lund University
Supervisor: Anna-Lena Sahlberg
Co-supervisor: Emilie Krite Svanberg

June 2022

Abstract

GAs in Scattering Media Absorption Spectroscopy (GASMAS) is a technique to study free gas inside strongly scattering bulk-materials. GASMAS is successful in safely measuring oxygen in lungs of neonates, with low-power tuneable diode-laser spectroscopy at 760 nm. Because a similar need of lung monitoring exists in older patients, this work explores how GASMAS can be scaled up for larger geometries. The major problem in large geometries is heavy light attenuation in tissue, making it necessary to increase the incident laser power. First, the performance of a low-power diode-laser GASMAS system was tested on wild boar lung. Next, an optical tapered amplifier (OTPA) was incorporated into the system with the goal of amplifying the light up to about 1 W. Finally, a high-power Titanium-Sapphire (TiSa) laser at 760 nm, not viable for practical GASMAS applications due to slow wavelength tuning, was used to study the level of light detection through tissue slabs, for varying slab thickness and laser powers. The results show a good oxygen signal through $3 - 5$ cm of lung tissue at 26 mW diode-laser power. The amplification of the diode laser light through the OTPA has not yet been fully successful, but the different parts of the system have been investigated and suggested optimisations were made for the future. With the high-power TiSa-laser, light of higher powers could penetrate through thicker tissue slabs. At 1 W, a good signal was detected through 14 cm of tissue, as compared to $3 - 5$ cm with 26 mW. In conclusion, the low-power diode-laser GASMAS system can detect oxygen in small lung geometries. Amplifying the power with an OTPA has good potential to enable oxygen GASMAS in large geometries. Future work should aim to better incorporate the OTPA into the diode-laser system with updated alignment equipment to amplify the power, in order to further investigate the applicability for GASMAS lung monitoring in larger children and adults.

II

Populärvetenskaplig sammanfattning

Hela livet är våra lungor livsviktiga organ. För nyfödda såväl som för äldre patienter så finns ett kliniskt behov av säker och kontinuerlig lungövervakning. Några av dagens vanliga metoder för att undersöka lungorna, såsom röntgen och datortomografi, ger endast en ögonblicksbild samt medför joniserande strålning. En ny teknik för klinisk lungmonitorering är nu på frammarch: GASMAS. GASMAS står för GAs in Scattering Media Absorption Spectroscopy, är fri från joniserande strålning och har potential att ge en kontinuerlig lungövervakning. Idag kan GASMAS framgångsrikt mäta syrgas i lungorna på neonatalt födda, där avstånden är små. Detta examensarbete tar nästa steg och studerar hur GASMAS kan skalas upp för större patienter.

Med gott resultat sattes ett GASMAS-system för syrgasmätning i lungor ihop. Systemet bestod av en diodlaser med kontinuerligt ljus vid 760 nm, för att matcha syrgasabsorption. Med låga lasereffekter om 26 mW genom en vildsvinslunga, kunde bra syresignaler uppmätas genom ca fyra cm lungvävnad. Om än förväntat så var detta goda resultat lovande inför att skala upp systemet för större geometrier! I större geometrier är den största utmaningen att det finns mer vävnad. Vävnad dämpar ljus kraftigt via både spridning och absorption. För att motverka detta så måste lasereffekten skruvas upp. Därför var nästa steg att förstärka laserljuset, samtidigt som det befintliga och framgångsrika GASMAS-systemet behölls intakt. För detta ändamål inkorporerades en optisk halvledarförstärkare. Förstärkaren hade en tre mikrometer stor ingångsyta mot vilken laserstrålen riktades. Lyckligtvis nog förstärktes det laserljus som träffade ingångsytan, men tyvärr var det blott en mycket liten del av det totala laserljuset. Utmaningen var att tre mikrometer är en sannerligen pytteliten öppning (ett hårstrå är ca 50 mikrometer tjockt). För att få ett GASMAS-system med bättre förstärkning, bör framtida studier fortsätta arbetet med att inkorporera förstärkaren. Att nå högre lasereffekter är kritiskt för målet om säker GASMAS-monitorering av större lungor. För att verifiera att högre lasereffekter verkligen tillåter ljuspenetration i tjockare vävnad, användes ett högeffektsystem med kontinuerligt ljus vid 760 nm. Detta system kunde inte användas till GASMAS, men det var passande för att studera ljuspenetration genom vävnad av olika tjocklek. Som vävnadsmodell användes lättskivade kasslerbitar. Resultaten visar att det mycket riktigt lönar sig att öka lasereffekten; med två Watt kunde ljuset penetrera hela 14 cm vävnad!

Det här examensarbetet har baserat på befintlig forskning konstruerat ett GAMAS-system med låg effekt för att undersöka syrgashalten i lungor över korta avstånd. För att använda systemet i större geometrier så behöver effekten skruvas upp. Nästa viktiga utmaning är därför att förstärka effekten genom att bättre inkorporera en optisk förstärkare. På så sätt så är detta arbete ett steg mot säker monitorering av lungor för fler patientgrupper.

IV

Acknowledgements

VI

Abbreviations

ASE	Amplified Spontaneous Emission
CW	Continous-Wave
FWHM	Full Width at Half Maximum
GASMAS	GAs in Scattering Media Absorption Spectroscopy
ND	Neutral Density
NTC	Negative Temperature Coefficient
OTPA	Optical Tapered Amplifier
SNR	Signal-to-Noise Ratio
TDLAS	Tunable Diode Laser Absorption Spectroscopy
TiSa	Titanium-Sapphire
WMS	Wavelength-Modulation Specotrscopy

VIII

Contents

X

1 Introduction

1.1 Background

Many materials contain pockets of free gas. Studying free gas that exists inside a denser bulk-material is of interest in multiple fields. A non-invasive optical technique that can be used to study such gas, is *GAs in Scattering Media Absorption Spectroscopy* (GASMAS). While light absorption peaks of free gas can be very narrow in wavelength, a solid or liquid bulk-material has broader absorption bands. Spectral absorption features of free gas inside strongly scattering bulk media can be sharp and distinct, like a needlestick, among the broader absorption features of the scattering bulk-material. This is critically utilised in GASMAS [1]. With GASMAS, it is for example possible to study oxygen levels inside food packages to investigate whether the package is sealed properly [2][3]. Moreover, GASMAS can be used to analyse the porosity of pharmacological tablets [4]. In other words, GASMAS is a spectroscopic technique with a variety of applications, probing gases that are surrounded by strongly scattering media [1].

This thesis is focused on a medical GASMAS application: the study of oxygen gas in lungs. Previous research has demonstrated the potential of GASMAS to study oxygen in the lungs of neonatal infants. This can be done non-invasively, using tunable diode-laser systems. These diode-laser systems emit light at 760 nm, which matches oxygen gas absorption [5][6][7]. Considering that the lungs are among the last organs to develop during pregnancy, there is indeed a need for safe lung monitoring in prematurely born infants [5]. Because a similar need for safe lung monitoring exists for older and larger patients as well, it is relevant to investigate how the lung monitoring GASMAS-technique can be scaled up for the larger geometries found in older patients [8].

A major challenge with oxygen GASMAS in large geometries is that the light becomes heavily attenuated. Biological tissue strongly attenuates the light by scattering and absorption, making light detection difficult over long path lengths. In a GASMAS study by Lin et al. (2021) [8], it is hypothesised that it is possible to compensate for the strong attenuation in biological tissue by increasing the power of the incident laser light. So far, the diode-laser systems achieving oxygen GASMAS-measurements in lungs have been of low power [6][7]. A potential way to increase the power of such a GASMAS system is to use an *Optical Tapered Amplifier* (OTPA); a diode with potential to greatly amplify the power of the seed laser while still preserving the input wavelength. The motivation for choosing an OTPA for power amplification is that the core of the present GASMAS system could be kept intact, preserving the tunable diode-laser system and associated signal-enhancing techniques that are already in place [8].

In approaching GASMAS for larger geometries, several challenges arise. To start with, it is valuable to study the performance and limits of current GASMAS systems. Furthermore, it is relevant to explore how an OTPA can be incorporated into the present system, with the goal to amplify the power. In addition, it is of interest to investigate how the power affects light transmission through biological tissue. In order to up-scale GASMAS for large geometries, these three perspectives are relevant to study.

1.2   Aims and Questions

With the overall purpose to contribute to the knowledge of how GASMAS can be scaled up for oxygen gas measurements in larger geometries, this thesis aims specifically to:

1. Set-up and test the performance of a low-power tunable diode-laser system by performing GASMAS. How well can oxygen GASMAS signals in lungs be detected? What are the limits of the current system?

2. Explore how an OTPA can be incorporated into the low-power tunable diode-laser system, with the objective to amplify the power of the laser light. What are the critical aspects in order to achieve optimal amplification?

3. Investigate how well laser light of 760 nm that is sent through biological tissue can be detected, for varying laser powers and tissue thicknesses. How well can light penetrate through tissue of increased thickness, if the power is increased?

1.3   Work Overview

The thesis work began with research into the theory and previous applications of GAS-MAS. In order to give some theoretical background to the topics of this thesis, chapter 2 presents basic concepts in tunable diode-laser spectroscopy, oxygen gas absorption, light attenuation in biological tissue, signal-enhancing wavelength modulation, lasers and OPTA:s.

The experimental work started with setting up and characterising a low-power tunable *Continuous-Wave* (CW) diode-laser system, with a central wavelength at 760 nm. GAS-MAS measurements were initially tested on styrofoam. Styrofoam was chosen as a test material because it is a strongly scattering and porous material with low light absorption at 760 nm. Then, GASMAS measurements were performed on a wild-boar lung filled with air. In addition, the temporal photon scattering inside the lung was studied with a pulsed dye-laser system, also at 760 nm. The work related to these GASMAS measurements is presented in chapter 3.

The next step was to explore how to incorporate an OTPA into the CW tunable diode-laser system (chapter 4). This required careful alignment and diffraction limit considerations. The critical aspects for the OTPA to function in the system and amplify the laser power were investigated in order to determine the most optimal system setup.

The last experiment (chapter 5) explored how deep into tissue that light of 760 nm can penetrate, for varying powers. Here, a CW *Titanium-Sapphire* (TiSa) laser was used that could reach powers up to 2 W, whereas the diode-laser system reached powers only up to 50 mW. In contrast to the diode-laser, the TiSa-laser wavelength cannot be scanned fast enough for GASMAS measurements. Therefore, this system was only used to investigate the light penetration. The TiSa laser light was directed onto a slab of pork, which was used as a simple model of scattering biological tissue. The light transmitted through the slab was measured. The laser power and slab thickness was gradually varied, studying how tissue thickness affected the level of light transmission.

The report concludes with an overall analysis in chapter 6, combining perspectives from the GASMAS measurements, the OTPA and the tissue slab measurements. Finally, an outlook is given that proposes future work within the field.

2 Theory

In this chapter, the theoretical concepts behind the main topics of this thesis are presented. The purpose is to provide background context to the upcoming discussions about the methods employed in oxygen GASMAS measurements in lungs.

2.1 Tunable Diode-Laser Absorption Spectroscopy

The systems for GASMAS are based on *Tunable Diode-Laser Absorption Spectroscopy* (TDLAS) [1]. Therefore, an overview of TDLAS is given here. Generally in laser spectroscopy, laser light is used to get information about properties of a sample. The laser light is directed, possibly with the help of optics, towards a sample volume. Inside the volume, the light can interact with the sample, after which its intensity is measured with a detector. In absorption spectroscopy, the sample is expected to absorb one or multiple wavelength/s of the light, attenuating the laser light. The absorption is wavelength-dependent. Tunable absorption spectroscopy means that the wavelength is tuned, scanned, over a range of different wavelengths. A decrease in the the measured intensity at the detector is then assumed to be a consequence of absorption at that particular wavelength. This way, a spectrum is attained that reflects the light-sample interactions for different wavelengths. By studying the spectral features, which are specific to the investigated sample properties, it is possible to get information about the sample ([9] p. 138, [10] p. 294 [11] p. 414). A schematic set-up for tunable absorption laser spectroscopy is illustrated in Figure 1.
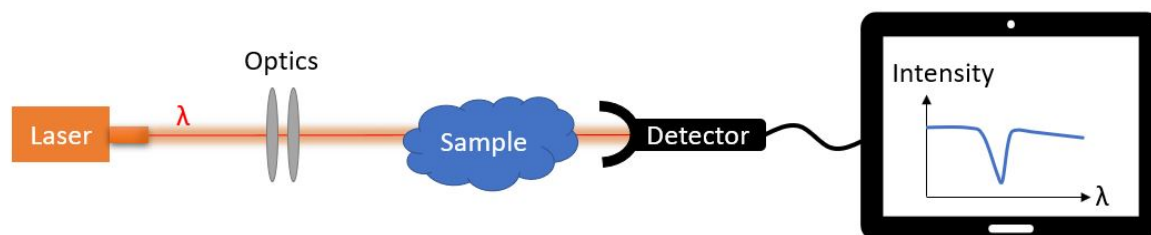
Figure 1: Schematic illustration of a set-up for tunable absorption laser spectroscopy. The laser light can be directed with the help of optical components into a sample volume. A detector measures the emerging light, whereafter a spectrum can be obtained. A decrease in transmitted intensity is measured when the wavelength λ corresponds to an absorption line.

TDLAS is considered as a form of absorption spectroscopy, where the tunable laser is a diode laser. A brief introduction to lasers is presented in section 2.5. Diode-lasers have

the advantage of easy and fast wavelength scanning [10]. In the form of TDLAS applied
in this thesis project, the wavelength is scanned triangularly up and down. The triangular
wavelength ramping also entails an associated triangular power ramping, this is further
discussed in section 2.5. If the laser light is measured with a detector, a triangular shape
reflecting the laser output-power is seen. If the wavelength-scan passes an absorption line
of the investigated sample, some of the laser light will be absorbed. The absorption is
seen as depressions in the detected intensity at the absorption wavelengths. The detected
intensity can be translated into sample absorption by subtracting the depressions from
the expected trend without the sample. The situation is illustrated in Figure 2.
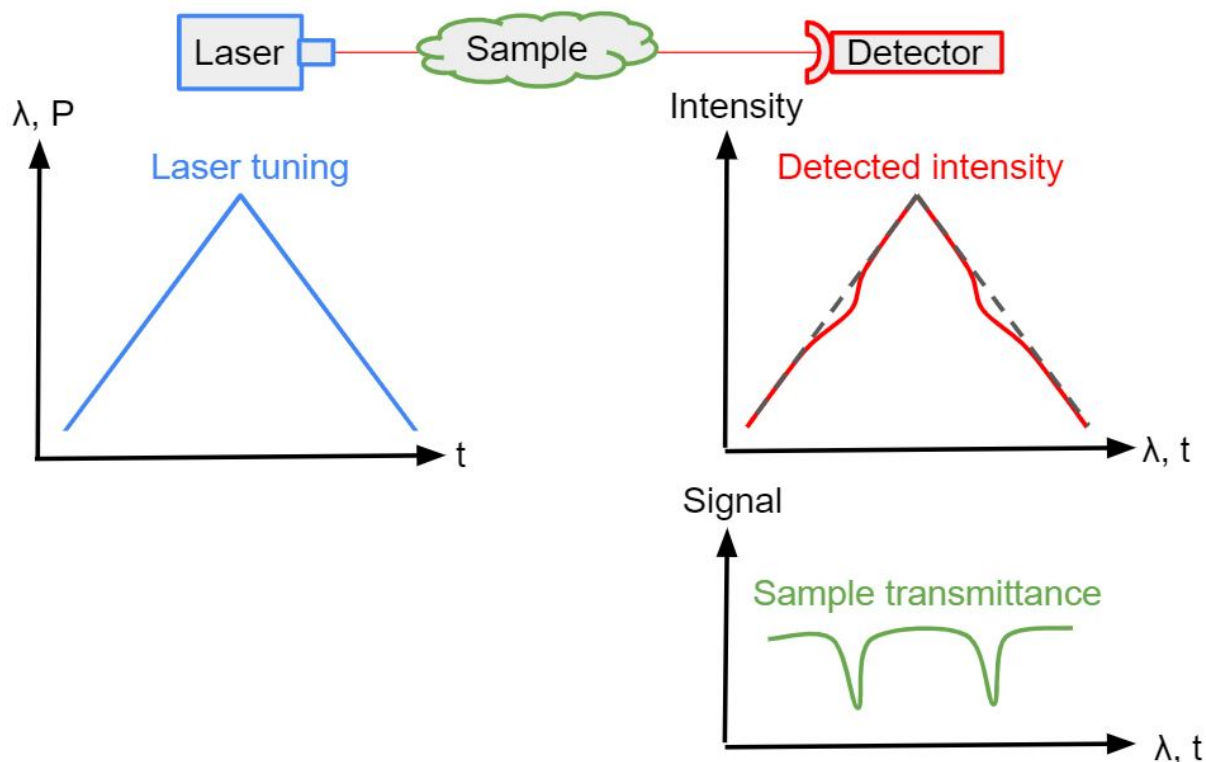
Figure 2: A diode-laser is tuned by triangularly ramping the wavelength λ in time (blue
curve). The wavelength-ramping is associated with a power (P) ramping. If the
laser is directed towards an absorbing sample, a detector can measure the
transmitted intensity (red curve). The intensity shows depressions at the
absorption wavelengths. In the illustration above, a dashed grey triangle marks
the expected detected intensity trend without absorbing sample. The sample
transmittance (green curve) can be found by subtracting the detected intensity
(red curve) from the expected trend (grey dashed curve) without the sample.

Depending on the application of TDLAS, the absorption imprint can be very small. This
is the case in GASMAS, where only a small fraction of the emitted laser light is captured
by the detector due to strongly scattering media. Therefore, signal-enhancing and noise-
suppressing techniques are used, in order to increase detection sensitivity. These include
Wavelength Modulation Spectroscopy (WMS) and lock-in techniques [1].

2.2   Techniques for Increasing Detection Sensitivity

Because the absorption imprints that are probed in GASMAS often are small [1], it is beneficial to use techniques that enhance the *Signal-to-Noise Ratio* (SNR). In this context, WMS and lock-in detection will be discussed next. Moreover, a short section about interference fringes is also included.

2.2.1   Wavelength Modulation to Enhance Sensitivity

In spectroscopic measurements, there are different noise-types that are relevant to consider. For GASMAS, one of these is the so-called 1/f-noise. This type of noise resides mainly in low frequencies. By pushing the detection towards higher frequencies, the impact of 1/f-noise can be lowered. WMS is a technique that is used for this purpose, by introducing high-frequency modulation of the laser light. The theory of WMS is vast and can be read more about in [12][13]. Here, a short overview of how WMS was used in this thesis is given.

In WMS, the laser wavelength is scanned at a high frequency of about 9 kHz on top of the base wavelength tuning of about $5 - 25$ Hz. Like the base wavelength tuning, the 9 kHz wavelength-modulation is also triangularly ramped up and down. The laser wavelength is then scanned over a target absorption-line. When the centre-wavelength of the laser matches a "slope" of an absorption line, the wavelength oscillation coming from the modulation leads to an amplitude oscillation in the detected signal. The magnitude of the amplitude modulation depends on how "steep" the slope of the absorption line is. As consequence, as the laser is tuned and modulated over an absorption line, the magnitude of the amplitude oscillation will vary. This amplitude oscillation occurs at the same frequency as the 9 kHz modulation and at higher harmonics of it.

In order to extract one frequency component of the WMS-signal, containing many harmonics of the 9 kHz-modulation, lock-in detection is used. Lock-in detection is a technique for extracting the amplitude of a component with a certain frequency. In GASMAS, lock-in detection is often employed to extract the second harmonic of the WMS-signal, the so called 2f-signal.

The intricate relation between base wavelength tuning, high-frequency modulation, absorption and 2f-signals is illustrated in Figure 3.
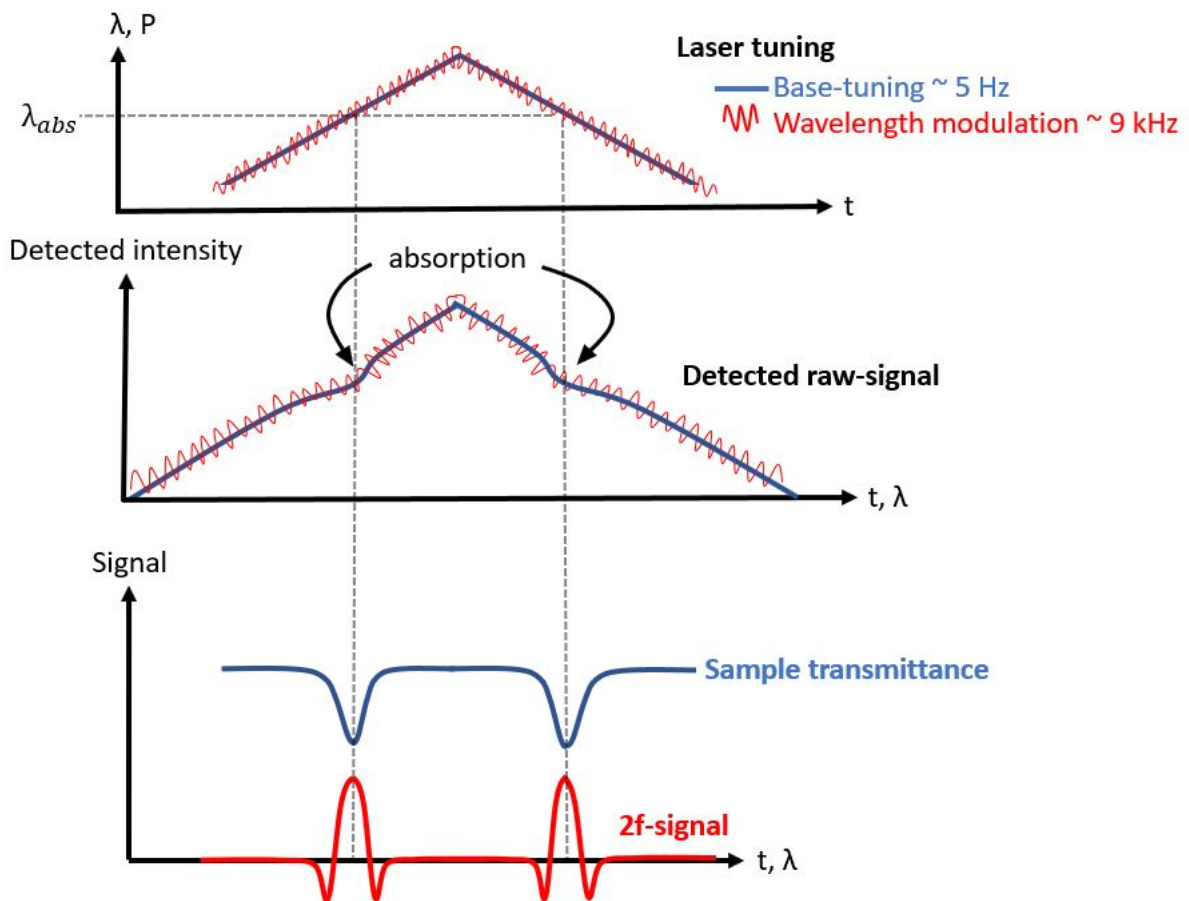
Figure 3: In direct absorption spectroscopy (blue curves), the base laser wavelength is triangularly scanned with a frequency of about 5 Hz (top graph). This results in an absorption at λ_{abs} which is visible as depressions in the detected raw-signal (middle graph). These depressions can then be translated to reflect the sample transmittance (blue bottom graph). In Wavelength-Modulation Spectroscopy (WMS), the laser is modulated at an even higher frequency of about 9 kHz (red graphs), on top of the base tuning (top graph). The detected raw-signal follows the same depression patterns reflecting absorption (middle graph). If lock-in detection is used, the signal-amplitude of the second harmonic of 9 kHz can be extracted as the $2f$-signal (bottom plot), which shows sample absorption. In the bottom graph, the red 2f-signal is approximately the second derivative of the blue transmittance-curve.

As a final comment on the theory of WMS, the modulation depth is important to discuss. The modulation depth corresponds to how much the wavelength is changed during one 9 kHz WMS-scan. If the modulation depth is too large, so that the wavelength sweeps well over an entire absorption line, the 2f-signal will be broadened. If however the modulation depth is too small, the resulting amplitude oscillation will also be small. This way, finding a suitable modulation depth resulting in high peak amplitudes is beneficial.

8

2.2.2   Avoiding Interference Fringes

Interference fringes is a relevant problem to discuss in relation to diode laser absorption spectroscopy. It can be read about thoroughly in [14], here only an overview is given. Due to parallel surfaces in the optical axis of a spectroscopic set-up, interference fringes may occur. The interference is caused by coherent superposition of light that is reflected multiple times by the parallel surfaces. Depending on the wavelength and path-length of the light, this causes either constructive or destructive interference, leading to unintentional modulation of the signal intensity. An example is shown in Figure 4, where the triangular ramping of the diode-laser is affected by fringes during WMS oxygen GASMAS measurements. The triangle is expected to not display these undulating edges.
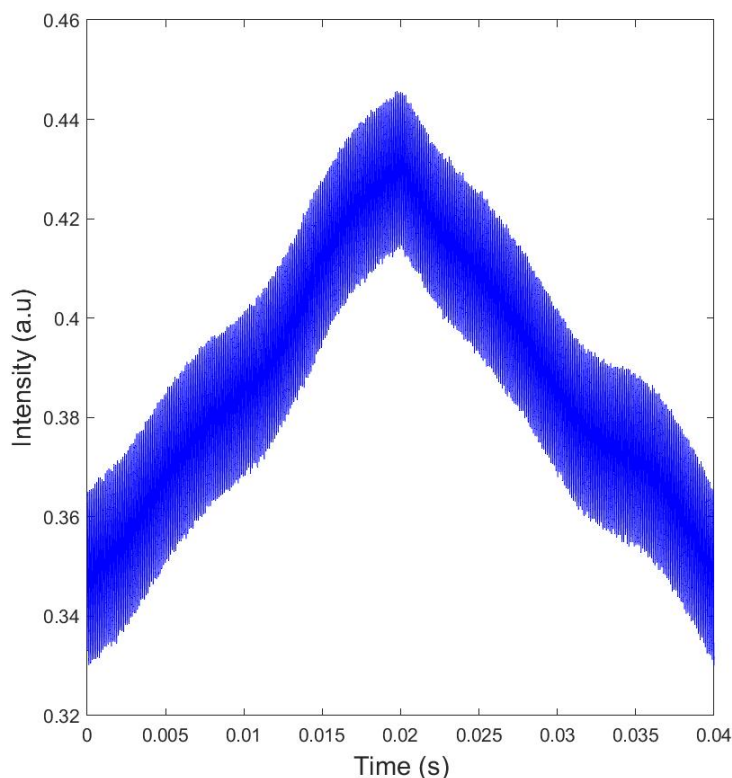
Figure 4: Interference fringes on the triangular ramping of a diode-laser, which is expected to have straight edges.

To counteract undulating interference fringes, some part of the laser-equipment can be shaken to introduce random perturbations which move the fringe locations. If also averaging is applied, interference fringe impact is decreased since the random variations disappear in the averaging process.

2.3   Spectral Lines of Oxygen Gas

In oxygen GASMAS, molecular oxygen gas is probed. In molecular spectroscopy, the spectral lines can result from transitions related to electronic, rotational and vibrational energy structures ([10], pp. 30 - 37). Considering oxygen gas, gaseous oxygen molecules

can absorb light that has a wavelength of 760 nm due to rotational-vibrational energy structures [1]. The transition intensities in the range from 760 nm - 762 nm are presented in Figure 5, in room-temperature at standard atmospheric pressure. An absorption line is centred on each one of these lines, with a certain line-width [10].
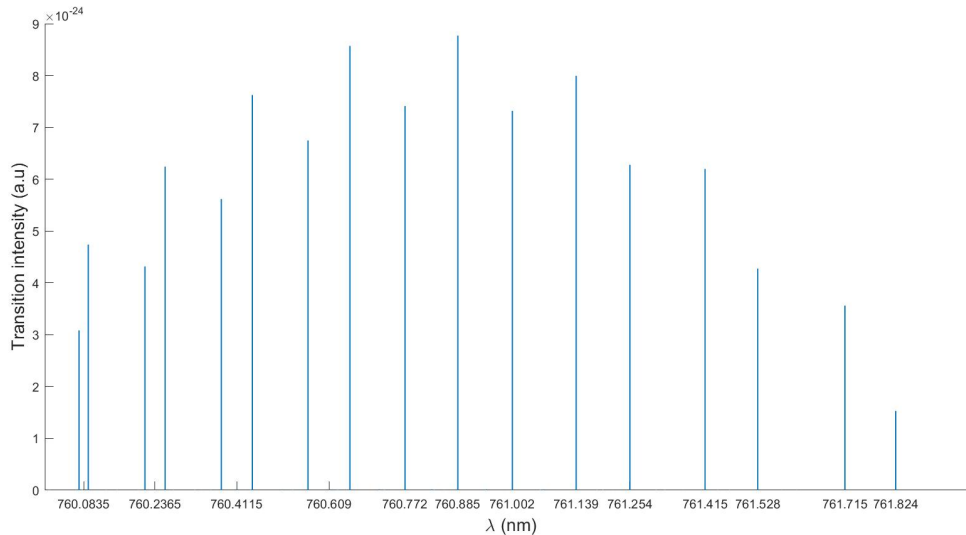
Figure 5: The major transition intensities of molecular oxygen gas. Plotted based on data from Hitran [15] that was retrieved by engineering master student Emma Hjörneby (Lund University, May 2022), with permission.

2.4   Basic Principles and Challenges of GASMAS

2.4.1   Spectrum of Free Gas in Scattering Media

In GASMAS, gas species that are surrounded by strongly scattering media can be investigated via absorption spectroscopy. The laser light enters the scattering bulk-medium. Some light is scattered and some may be absorbed by the bulk material. Parts of the light will pass through to gas pockets and interact with the target gas. It is expected that only a small portion of this light that has interacted with the gas will be detected at the detector [1].

The energy-bands of free gas molecules result in sharp spectral features, whereas the structures of denser and more complex materials give rise to broader spectral features. This means that spectral features of free gasses can be distinguished from those of the surrounding host-material [1]. Illustrated spectra from a scattering bulk-material, free gas and a porous bulk-material are shown in Figure 6.

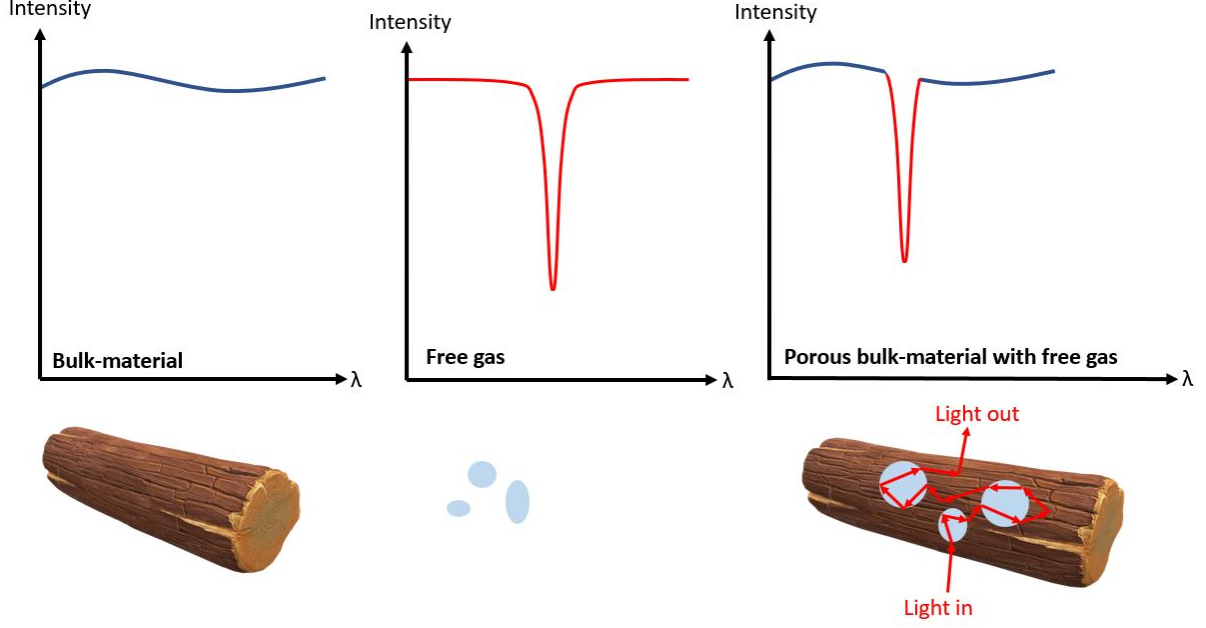**Figure 6:** The schematic absorption spectra of a strongly scattering bulk-material (left), free gas (middle) and a porous bulk-material (right) are presented. In the right-most image, the situation of Gas in Scattering Media Absorption Spectroscopy (GASMAS) is shown. Illustration adaption inspired by Figure 2 and Figure 3 in [1].

2.4.2 Challenges with Unknown Optical Path Length

Because GASMAS is a type of laser absorption spectroscopy, it is relevant to discuss the Beer-Lambert law, which describes how the light from a laser is attenuated when travelling through a sample [1] ([9] pp. 127 - 128). After an optical path-length L, the laser light intensity is given by the Beer-Lambert law as:

$$I(L) = I_0 e^{-\sigma N L} \tag{1}$$

where I_0 is the laser light intensity before absorption, N is the number density of the absorbing particles and σ is the absorption cross-section [1] ([9] pp. 127 - 128). Before applying the Beer-Lambert law in Equation 1, a problem with GASMAS is that L is not well defined due to the strongly scattering host-material. Of those photons that are detected at the detector, some photons will have propagated long and some short optical path lengths inside the sample [1].

There are different ways of working with an unknown optical path length in absorption spectroscopy. One way is to study a reference gas apart from the target gas, with a wavelength very close to the target wavelength. If the interrogating wavelengths of the target and reference gasses are very close, then it may be possible to assume that light of these wavelengths travel about the same path length inside the sample medium. If moreover the number density and absorption cross section of the reference gas is known, then an approximate mean value of L for the reference gas can be computed from absorption spectroscopic measurements of the reference gas. By assuming that the gases

have the same expected optical path length, the number density can be computed for the target gas (if its absorption cross section is known) [1]. For example, consider Equation 1 with a reference, ref, gas that is probed with λ^{ref} and a prime $target'$ gas that is probed with $\lambda' \approx \lambda^{ref}$. For the reference gas, it is assumed that N^{ref} is known, I_0^{ref} and μ^{ref} are also known and I^{ref} can be measured. Thereby, the only unknown parameter in Equation 1 is L^{ref} which can be computed. Next, it is assumed that $L^{ref} \approx L'$ because $\lambda' \approx \lambda^{ref}$. If now I' is measured and I'_o, σ' and L' are assumed to be known, then the number density N' for the target gas is given by Equation 1.

For oxygen GASMAS purposes, a possible calibration gas is water vapour. If the relative humidity is 100 %, then the number density of water vapour depends only on the temperature. Inside lungs, the relative humidity is indeed expected to be about 100 %, whereby the water vapour number density is known at 37 °. With water vapour as a reference gas, the number density of oxygen can be investigated with GASMAS [1].

Generally, an important goal of oxygen GASMAS is to get information about oxygen gas concentrations [1]. However, no reference gas measurements are done in this thesis work, making it impossible to get information about absolute concentrations with the techniques used. Here, the focus lies instead on exploring the ability to detect any GASMAS-signals at all, rather than interpreting those signals and translating them into concentrations.

2.4.3   Scattering and Absorption in Biological Tissue

With oxygen GASMAS in lungs, light scattering and absorption in biological tissue is relevant to discuss. Light is strongly attenuated through scattering and absorption in biological tissue. The therapeutic window is a wavelength-range where tissue on the other hand is relatively transparent, making these wavelength range suitable for GASMAS. The tissue optical window ranges from about 650 - 1350 nm ([9] pp. 126 - 130). In light of the range of the tissue optical window and the specificity of oxygen gas to absorb at 760 nm, this is a suitable wavelength.

In this report, "biological tissue" is referred to in a general sense without specifying tissue type. Tissue type may however have implications on light scattering and absorption properties, possibly affecting light propagation in tissue ([9] pp. 126 - 131). As a limitation, only in a broad sense is biological tissue referred to here; differences between optical properties of different tissue types are not regarded.

2.5   A Brief Introduction to Lasers

Because GASMAS is based on laser spectroscopy, a brief introduction to the laser types used in this thesis work is given here. Laser stands for *Light Amplification by Stimulated Emission of Radiation.* Generally, a laser consists of a cavity in which there is a laser-medium and reflecting mirrors as cavity walls. The laser-medium is pumped (supplied with energy) to create a population-inversion. Population inversion means that electrons get lifted from a lower to an upper state, so that the upper state is more populated than the lower. *Amplified Spontaneous Emission* (ASE) means that an excited electron can spontaneously be de-excited down to a lower state from an upper, resulting in emitted

electromagnetic radiation. In contrast to spontaneous emission, there is also stimulated emission. When a photon enters a population-inverted laser-medium, and if the photon energy matches the energy between the lower and upper state, the excited electrons are stimulated to de-excite and return to the lower state. In this stimulated de-excitation, electromagnetic radiation is emitted. The emitted photons have the same wavelength as the incoming photon ([10] pp. 227 - 235). The laser-medium is moreover placed in a resonator for feedback, which is made up by the reflecting mirrors at the cavity walls. As light is reflected between the mirrors, the intensity is increased. Furthermore, in order to obtain a laser beam, one of these mirrors is partly transparent to emit output-light in one direction. In addition, because the cavity has a fixed length and reflecting walls, photons are restricted due to interference by multiple reflections. As a result, only light with wavelengths that satisfy conditions for constructive interference can survive in the cavity ([10] pp. 227 - 235).

There are many different types of lasers. In diode-lasers, the laser-medium is composed of semiconductor materials. Here, population-inversion is achieved via a driver current, and the lasing occurs at the transition zone of a pn-junction. Applying a voltage over the junction forces holes and electrons into the transition region, whereby stimulated photon emission can take place when holes and electrons recombine. The emitted photon energy matches that of the band-gap. Regarding tuneability, rapid fine-tuning of the wavelength can be done through scanning the driver current, which also changes the laser power. For coarse wavelength tuning, changing the temperature changes the refractive index of the laser-cavity, resulting in coarse tuning. Because the diode laser cavity is quite small, diode lasers can lase at a single frequency ([10] pp. 259 - 261).

In dye lasers, laser action takes place in organic dyes. If the dye is pumped in pulses, for example by a pulsed laser, a pulsed dye laser system can be obtained. Different output-wavelengths are viable by using different types of dye, ranging from 260 nm up to 900 nm ([10] pp .246 - 252).

The TiSa-laser has a lasing medium of Titanium-doped Sapphire, enabeling output wavelengths of about $660 - 1100$ nm ([10] pp. 256 - 257). This is an example of a solid-state laser that is optically pumped ([11] p. 284).

2.6   Optical Amplifier

Light from a laser can be amplified with a semiconductor optical amplifier, whose structure is similar to that of a laser. An optical amplifier also has a gain medium, but no cavity with reflecting walls like a laser. The gain medium is a crystal. Via a current, population inversion is achieved in the gain medium and there is spontaneous emission of polychromatic light. The light is polychromatic because there is no cavity with reflecting walls. Light that enters the cavity will stimulate emission of light of the same wavelength, leading to stimulated amplification. This means that the amplification works for only light with the same wavelength as the input seed-laser wavelength. For this process to be optimal, the incoming seed-laser light must be perfectly aligned with the gain direction [16].

3 GASMAS Measurements in Wild Boar Lung

In this chapter, GASMAS measurements with a tunable diode-laser system are presented. The purpose with these measurements was to test if the diode-laser system can detect oxygen GASMAS signals in lungs. The system components had not been in active use for considerable time, motivating the need to test the system performance in a GASMAS-setting, despite previous research [5][6][7] that has already shown that tunable diode-lasers are suitable for oxygen GASMAS lung measurements. First, the diode-laser system was set up and characterised by performing GASMAS measurements on styrofoam. Similar to lungs, styrofoam scatters light strongly and contains free oxygen gas that can be probed with GASMAS. Styrofoam also has low absorption at the oxygen-interrogating wavelength of 760 nm, making it a suitable test-material. Having characterised the system on styrofoam measurements, GASMAS measurements were done on wild boar lung.

In addition, a pulsed dye laser system is also introduced in this chapter. Compared to the low-power diode-laser with powers below 50 mW, the pulsed system delivers pulses with peak pulse energies in the MW-range. Measurements were done on lungs with the pulsed system with the goal of investigating the temporal photon scattering inside lung tissue. Because the pulsed light has higher power than the CW light of the diode-laser, it would be beneficial if this high-power pulsed light could be used in GASMAS-setups, especially in large geometries. A previous study [8] has used a high-energy pulsed system to study the light scattering in styrofoam, where also the oxygen concentration inside the styrofoam could be assessed. However, no successful recordings could be retrieved when the pulsed system was applied on biological samples such as chicken. The study also discusses the many challenges associated with high-energy pulsed systems for GASMAS. For example, using high-energy pulses in a clinical context may raise safety regulation concerns. Moreover, pulse-to-pulse fluctuations can result in uncertain detection. Some pulsed laser systems can also be bulky in comparison to small diode-lasers, reducing the applicability. Due to these challenges and because previous research [5][6][7][8] show that tunable CW systems are promising in GASMAS-setups, the pulsed dye-laser system will not be discussed in great detail here. However, pulsed GASMAS-measurements on lung tissue have not been introduced before in this research area, making such measurements interesting nevertheless.

With the GASMAS-measurements, it was possible to evaluate the diode-laser system. The measurements also enabled GASMAS-signal comparison between the pulsed dye-laser and the CW diode-laser. The findings motivates continuous work with the diode-laser system for future GASMAS-settings.

3.1 The Diode-Laser System

The following sections present GASMAS measurements with a diode-laser system, which was based on a CW tunable single-frequency distributed feedback diode-laser, emitting low-power light with a central wavelength of 760 nm. This type of system has successfully been used in GASMAS-setups for oxygen gas measurements in lungs before [5][6][7].

3.1.1 Setup of the Tunable Diode-Laser

Laser and Laser Drivers

The tunable diode-laser (EYP-DFB-0760-00040-1500-BFW01-0005, eagleyard Photonics) emitted collimated CW light with typical output-powers around $10-35$ mW. The central wavelength was 760 nm to match an absorption peak in molecular oxygen gas [8]. The laser was connected to two laser drivers: a current driver (LDC 205 C, Thorlabs) and a temperature driver (TED 200 C, Thorlabs). A photography of the diode-laser, mounted and connected to laser-drivers, is presented in Figure 7.
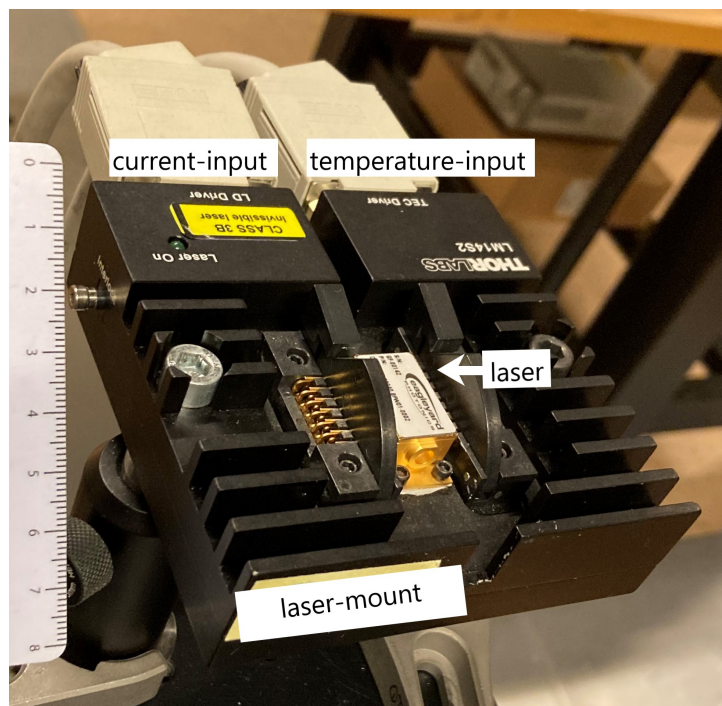

Figure 7: Photography of a distributed-feedback (DFB) diode-laser (YP-DFB-0760-00040-1500-BFW01-0005, eagleyard Photonics). The laser is mounted and connected to current (LDC 205 C, Thorlabs) and temperature (TED 200 C, Thorlabs) laser drivers. A cm-scale is visible to the left for reference.

The laser wavelength could be tuned by changing the laser driver current and temperature. Adjusting the temperature corresponded to coarse wavelength tuning, whereas changing the current could be used for rapid fine-tuning. The temperature was tuned by altering the resistance of a standard *Negative Temperature Coefficient* (NTC) thermistor. An increase in the thermistor resistance caused a decrease in temperature, while a

16

resistance decrease corresponded conversely to a temperature increase.

Software for Wavelength Tuning and Signal Detection

Software in LabView and Matlab enabled laser wavelength tuning and processing of detected signals. Via a LabView interface, the laser wavelength could be scanned by ramping the laser driver current. The laser driver current was set to base ramp triangularly up and down 25 times per second. The purpose of scanning the wavelength was to be able to detect increased absorption when the laser-wavelength coincided with an absorption line, and decreased absorption when the wavelength was scanned to a value outside the absorption peak. The detected signals were also processed in LabView.

In order to be able to detect weaker signals, WMS was used. Therefore, additional wavelength modulation was applied on top of the base tuning via Labview. This wavelength-modulation corresponded to ramping the laser driver current triangularly 9025 times per second. A ready-to-use Matlab script was used to compute the 2f-signal from the detected intensity signal.

The LabView and Matlab scripts were initially developed by Märta Lewander during her doctoral studies in physics, at the Department of Physics at Lund University. Lewander defended her PhD dissertation [17] in 2011. Since the year of 2011, the LabView and Matlab programmes have been slightly altered along the way by PhD students in physics at Lund University.

3.1.2   Characterising the Tunable Diode-Laser

Tuning the Laser Power

A power-meter (S302C, Thorlabs) was used to record the laser power for different values of laser driver current and laser driver thermistor resistance. It was found that increasing the laser driver current increased the output power, which is indicated in the left plot in Figure 8. The middle-plot in Figure 8 indicates how the temperature affected the output power. Moreover, a wave-meter (WS-5, HighFinesse) was used to study how the wavelength affected out-put power, which is described by the right plot in Figure 8. The wavelength was changed by randomly changing the values of both laser-drivers.
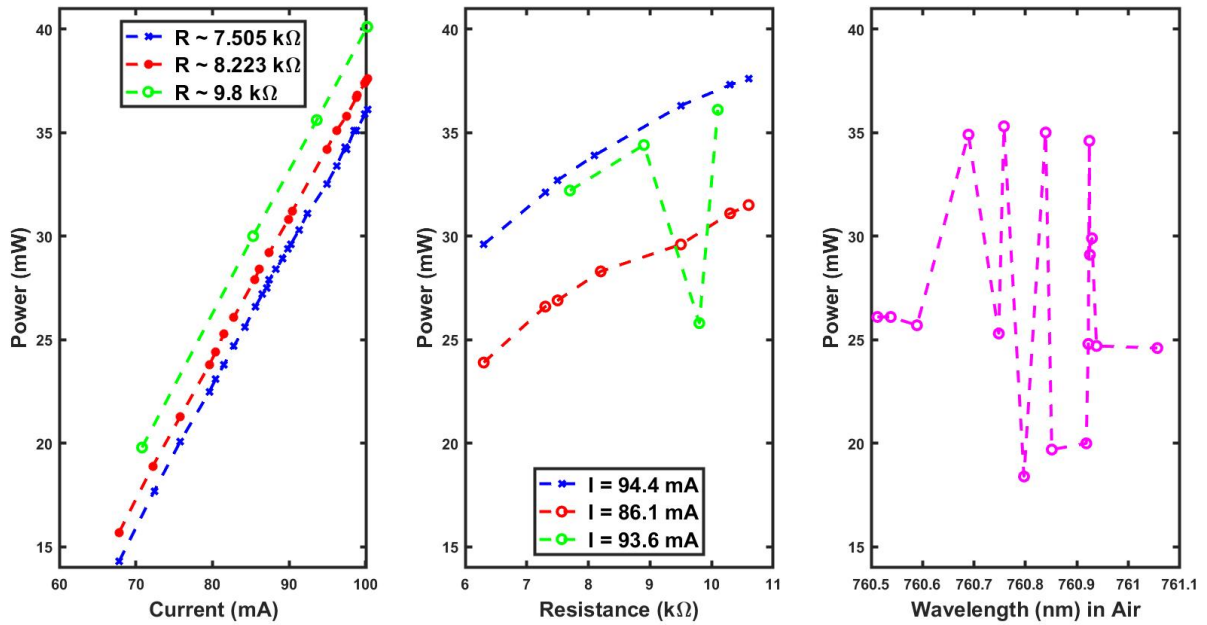
Figure 8: Output power from a continuous-wave (CW) distributed-feedback (DFB) diode-laser, for varying laser driver current (I), thermistor resistance (R) and out-put wavelength.

It is noted that changing the wavelength by changing the laser driver current also changes the laser-power. A triangular laser driver current ramp set via the LabView interface would thus correspond to a triangular power-ramp of the laser light.

Optimising Modulation Depth

Because GASMAS-signals are expected to be weak, WMS and lock-in techniques were applied. A parameter affecting the 2f signal-amplitude is the modulation depth. The modulation depth corresponds to how much the wavelength is changed during one modulation-scan. Therefore, it was important to optimise the wavelength modulation depth to obtain oxygen 2f-signals with high peak amplitudes. In order to obtain high peak amplitudes, the mean peak amplitude of a typical $2f$-signal was studied. The mean peak amplitude is the mean of the two maxmimum amplitudes in the 2f-signal. The wavelength modulation depth was optimised to maximise the mean peak amplitude of oxygen signals.

A piece of styrofoam (3.5 cm × 7 cm × 24 cm) was used as a sample in optimising the modulation depth. The light from the laser was directed onto the styrofoam and then detected behind the styrofoam with a photo-diode (DET210, Thorlabs). In the direction the input light, the styrofoam thickness was 3.5 cm. The setup to optimise modulation depth can be found in Figure 9.
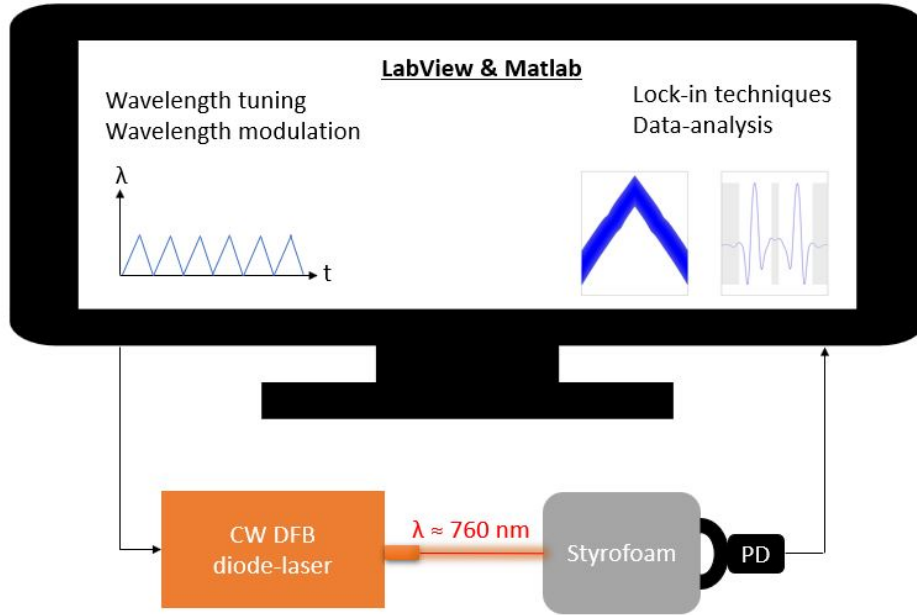
18

Figure 9: Set-up for optimisation of the wavelength-modulation depth in Wavelength-Modulation Spectroscopy (WMS), using a tunable Continuous-Wave (CW) distributed feedback (DFB) diode-laser with 760 nm central wavelength. The wavelength tuning and modulation was controlled via LabView. The light transmitted through a piece of styrofoam (3.5 cm × 7 cm × 24 cm), was detected via a photodiode (PD). Lock-in to extract the 2f-signal and data-analysis was performed in LabView and Matlab.

The mean peak amplitude of the 2f-signal was detected for varying values of modulation depth. The result is presented in Figure 10a, where the optimal modulation depth maximising the mean peak amplitude was 275 mV. The corresponding 2f-signal for this modulation depth is shown in Figure 10b.
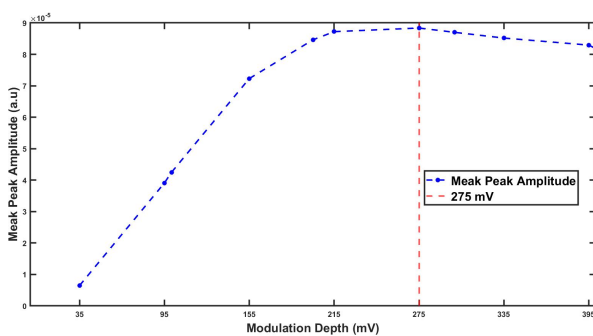
(a) Mean peak amplitude for different of modulation depths (mW).
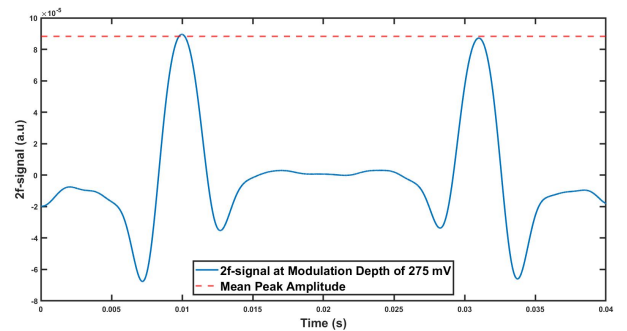
(b) 2f-signal (blue whole-drawn curve) and mean peak amplitude (red dashed line) at a modulation depth of 275 mV.

Figure 10: Meak peak amplitude and 2f-signal as found by wavelength-modulation spectroscopy (WMS) on styrofoam, with a tunable continuous-wave (CW) diode-laser with a central frequency of 760 nm.

Measured with the wave-meter, a modulation depth of 275 mV affected the third decimal of the laser-wavelength. For comparison, it was found with the wave-meter that the 25 Hz base wavelength tuning affected the second decimal of the laser-wavelength. In this context, it is noted that the base wavelength tuning has a depth of 300 mV, corresponding to a range of about $\Delta\lambda \approx 0.1$ nm per scan.

Having set up, characterised and tested the diode-laser system, GASMAS lung measurements were done next.

3.2   Oxygen GASMAS in Lungs with TDLAS

3.2.1   Experimental Set-Up for Diode-Laser Lung Measurements

Having optimised the modulation depth and tested the diode-laser through styrofoam measurements, the system was then used in oxygen gas GASMAS lung measurements. The setup for oxygen GASMAS in wild boar lung tissue is shown in Figure 11.
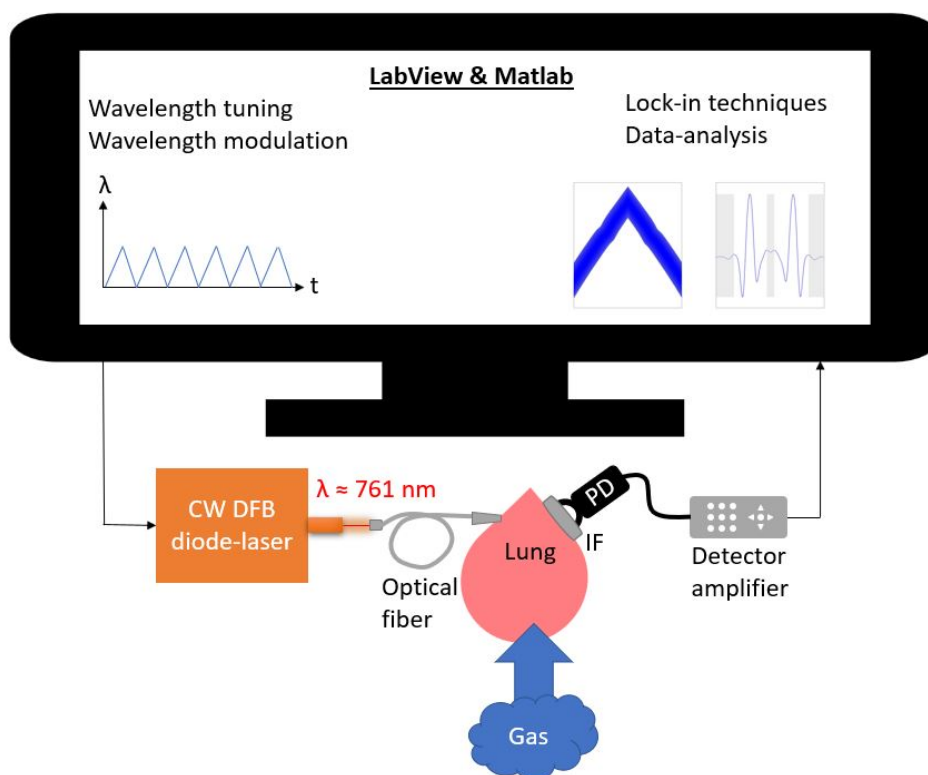
Figure 11: Set-up of a continuous-wave (CW) distributed feedback (DFB) diode-laser system for GAs in Scattering Media Absorption Spectroscopy (GASMAS). The wavelength was tuned and modulated via LabView, with a central value of 761 nm. The light entered an optical fibre and was administered into ex vivo wild boar lung tissue that was supplied with gas. The signal was detected with a photo-diode (PD). An interference filter (IF) placed before the detection area. After reaching the PD, the signal was conveyed via a detector amplifier to a computer. Lock-in techniques and data-analysis were done via LabView and Matlab.

The laser wavelength was tuned with a frequency of 25 Hz. In addition, wavelength modulation occurred with a frequency of 9025 Hz, using the optimal modulation depth.

Because the purpose was to probe the oxygen gas inside the lungs and not in the oxygen in the ambient air, the light path length in air was minimised. A simple optical fibre was placed at the laser output, collecting the laser light. The end-tip of the fibre was placed in close contact with the target lung tissue. The light exiting the fibre and entering the lung tissue was not collimated. To counteract the impact of interference fringes, the fibre was shaken during the measurements.

The target lung lobe was supplied with gas via an endotracheal tube and pumped with a bag valve mask. The supplied gas was either air (room-air) or nitrogen gas. The purpose of flushing air was to simulate breathing and probe the oxygen gas. When nitrogen was flushed into the lung tissue, it was expected that the oxygen partial pressure would decrease in favour of nitrogen, decreasing the oxygen signal [5]. In this way, flushing nitrogen was a way to investigate if the signals that were measured during air supply could be assumed to reflect absorption specifically from oxygen gas. The lung sample was about $3-5$ cm thick in direction of transmission from the output-tip of the optical fibre.

Laser light emerging from the lung tissue was detected with a photo-diode (S3590-08, Hamamatsu), which had a detector area of about 1 cm^2. A larger detector area was favoured in order to be able to detect more light. In order to block out ambient light from the room, probing detection of the laser light, an interference filter (FB760-10, Thorlabs) was placed before the detector area. This filter had a bandwidth to transmit light of 760 ± 10 nm. The detector with the interference-filter was placed directly onto the lung tissue, avoiding detection of ambient light form the room. Moreover, because the GASMAS-signals were expected to be weak, a detector amplifier (DHPCA-100, Femto) was connected to the detector.

The detected GASMAS signals were processed in the LabView programme. To avoid effects of interference fringes on the signals, random electrical noise was introduced by shaking the optical fibre. Moreover, averaging of 1000 scans was applied when recording the GASMAS-signals in the LabView interface.

Tuning the Wavelength to an Absorption Line

In order to verify that the central wavelength of the laser was tuned to an absorption line, the same set-up and procedure as depicted in Figure 11 was used, but with a piece of styrofoam (3.5 cm $\times$ 7 cm $\times$ 24 cm) instead of lung-tissue. The styrofoam measurement was done before starting the lung measurements, making sure to target an absorption line during the lung measurements described above. With styrofoam as test-sample, the laser-drivers were tuned so that an absorption could clearly be seen in the GASMAS-signal. The values of the laser-drivers were set to 7.505 kΩ and 94.89 mA, resulting in a central wavelength at 760.924 nm in air and 26 mW out-put power.

3.2.2 GASMAS-Signals from Lung Measurements with TDLAS

Representative plots from the diode-laser lung measurements are presented in Figure 12. For comparison, the styrofoam measurement is also displayed, which was carried out on the same experimental occasion and with the same setup as the lung measurements. The top triangular plots in Figure 12 display the detected light intensity at the detector. The bottom plots show the corresponding 2f-signal after WMS and lock-in. The grey fields mark the signal-parts that are assumed to be noise. The noise-parts were indicated by assuming that the signal would have a typical 2f-shape, and then identifying the highest peak in the first and the second half time interval. The signal besides these peaks were assumed to be noise. Regarding the measurement representing lungs with nitrogen gas supply, the same noise-identifying strategy was applied even if the signal does not resemble a typical 2f-signal.
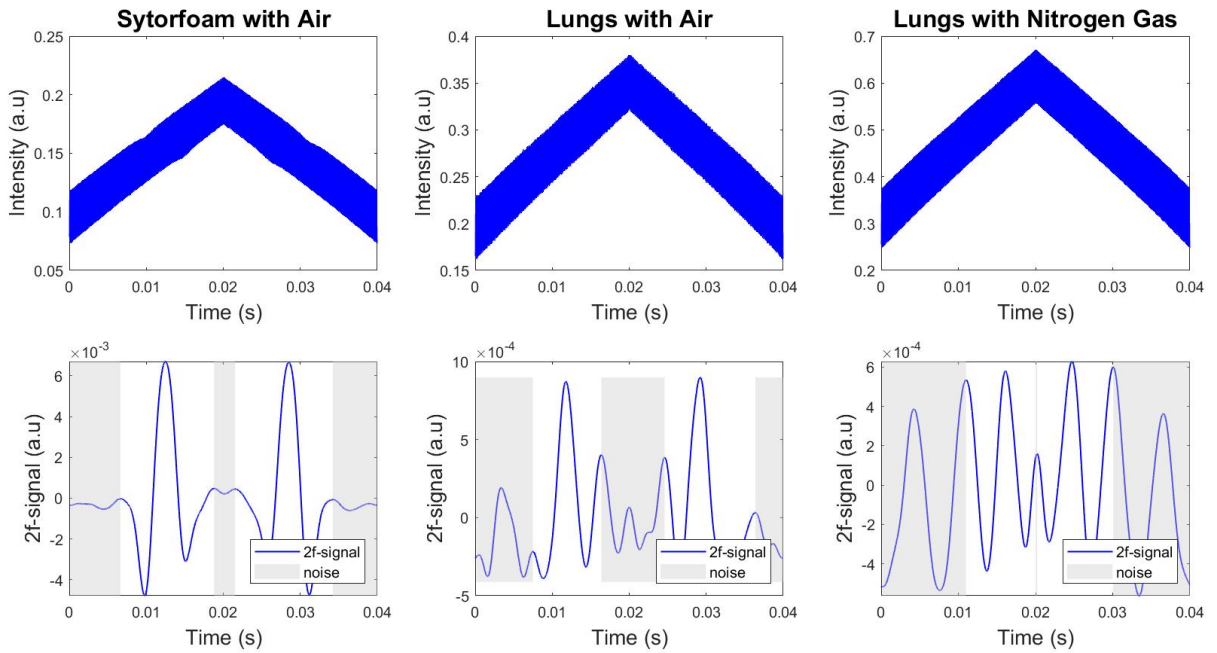

Figure 12: Representative plots from continuous-wave (CW) diode-laser measurements on styrofoam (left), lungs with air (centre) and nitrogen gas (right). The base wavelength of the laser was scanned 25 times per second, op top of which wavelength-modulation was employed at a frequency of 9025 Hz. The top plots represent the detected intensity, reflecting the wavelength sweep in time. The signal is the average of 1000 scans. The bottom plots show the 2f second harmonic signal after wavelength-modulation and lock-in detection.

In order to asses how well the experimental set-up was able to measure oxygen GASMAS-signals, it is relevant to investigate whether the detected signal first of all comes from the laser, and second if the signal reflects oxygen gas absorption.

First, the triangular shapes of the top plots i Figure 12 indicate that it is the laser light that is detected. To motivate this, it is considered that the laser driver current

22

was scanned triangularly during the measurements. The triangular ramp resulted in a wavelength-ramp but also in a power-ramp. Because the detected light emerging from the lung tissue displays a triangular intensity-ramp, it is indicated that the detected light comes from the laser. This suggests that the system was able to send light into the lung and then detect it in the photo-diode.

Second, the bottom 2f-signal plots in Figure 12 are studied in order to investigate if the signals represent oxygen gas absorption. If the signals represent oxygen, it is expected to find typical 2f-signals for measurements with air, but not with nitrogen gas. The reason for this is that flushing nitrogen gas is assumed to decrease the partial pressure of oxygen [5], resulting in a lower signal intensity if the laser light probes oxygen gas. Here, the styrofoam signal resembles a typical 2f-signal. The outline of such a 2f-signal can also be seen for the measurement on lungs with air, although noisier. However, the signal from lungs with nitrogen gas does not resemble a typical 2f-signal. Nitrogen flushed lungs are expected to display very low partial pressure of oxygen. There is however expected to be some residual oxygen inside the lungs that does not disappear when flushing nitrogen, why the nitrogen-signal reflects only a very small oxygen content. From this qualitative comparison, it is suggested that the 2f-signals do reflect oxygen.

To compare the signals also quantitatively, an SNR-value for the 2f-curves was defined and used for comparison.

3.2.3   Comparing 2f-Signals from GASMAS with SNR

In order to quantitatively compare 2f-signals, an SNR-value was defined as SNR $= 2f_{\mathrm{MPA}}/\mathrm{rms(noise)}$, where rms(noise) is the root-mean-square of the signal noise. In Figure 12, the grey fields indicate which parts of the signals that were assumed to be noise.

The SNR-values from the GASMAS measurements with the diode-laser system are presented in Table 1 (Appendix A). The mean (standard deviation) of the lung measurements were approximately 5 (1.8) with air ($n = 25$) and 2 (0.31) with nitrogen gas ($n = 4$) supply. The styrofoam measurement ($n = 1$) rendered an SNR-value of 17.7. The SNR-values in Table 1 are visualised in Figure 13.

From the SNR-values plotted in Figure 13 and the SNR-means (17.7 for styrofoam, 5 for lungs with air and 2 for lungs with nitrogen), it is noted that the SNR-values from lung measurements when flushing nitrogen gas were low. Due to the lower SNR-values from lung measurements with nitrogen supply compared to those with air supply, the 2f-signals in Figure 12 likely reflect oxygen. Again, it is noted that nitrogen gas flushed lungs are expected to have low partial pressure of oxygen, but the oxygen content is still expected to be above zero due to residual oxygen. This quantitative analysis indicates that the diode-laser system was able to detect oxygen GASMAS signals in lung tissue.

Regarding the lung measurements with air, SNR-values were expected to be higher than those for nitrogen but lower than that for styrofoam. In Figure 13, it is noted that the lung measurements with air resulted in SNR-values ranging from about 2.5 up to 9.6, overlapping neither with the SNR-range of the lung measurements with nitrogen

$(1.7 - 2.4$, $n = 4)$ nor with that of styrofoam $(17.7$, $n = 1)$. While it is not possible to draw absolute conclusions about whether the SNR-values were significantly different between the different groups, the tendencies are interesting.
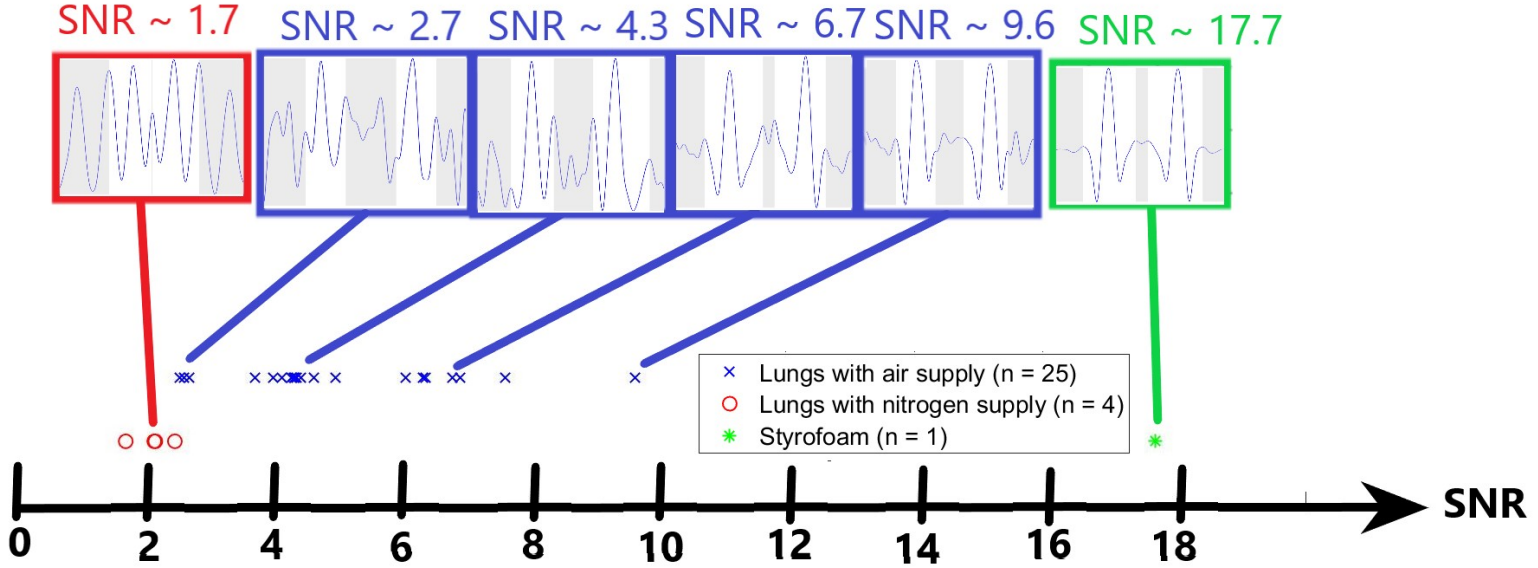

Figure 13: Signal-to-noise ratio (SNR) of measurements with a continous-wave (CW) diode-laser system used for oxygen GAs in Scattering Media Absorption Spectroscopy (GASMAS) on wild boar lung with air (blue crosses) and nitrogen (red circles) gas supply. The boxes with graphs next to the data points show representative plots of the 2f-signal, as found after wavelength-modulation spectroscopy (WMS) and lock-in detection. For comparison, a styrofoam (green star) measurement is also presented.

In summary, the representative plots from diode-laser GASMAS measurements in Figure 12 suggest that the laser system was able to detect the laser light emerging from lung tissue. Comparing the signals between measurements with air supply versus those with nitrogen supply, the plots in Figure 12 and the SNR-comparison in Figure 13 suggest that the GASMAS-signals attained actually reflect oxygen gas absorption - even of absorption of small residual gas amounts during nitrogen flushing. This way, it is demonstrated that laser light detection reflecting oxygen gas levels inside lung tissue was achieved with this diode-laser system.

3.3 Evaluating the GASMAS Diode-Laser System

The wild boar lung measurements tested the performance of the diode-laser system. The representative GASMAS-signals attained in Figure 12 and SNR-comparison presented in Figure 13, indicate that this tunable diode-laser system is able to perform oxygen GASMAS measurements on lungs. This was expected from previous research [5][6][7], and motivates continuous work with such a system for GASMAS purposes in the future.

The experiment described above showed that light from a diode-laser of 26 mW could penetrate through $3 - 5$ cm of lung tissue and give good signals in these geometries. For GASMAS in larger geometries, it is believed that higher powers are needed. As have already been discussed, amplifying the diode-laser light with an OTPA has been proposed by a previous study [8]. With an OTPA light-amplification, the main parts of the already existing diode-laser based GASMAS could be kept intact [8].

In addition, another way to test GASMAS with light at 760 nm at high powers is presented in the next section, introducing a high-power pulsed dye-laser system. Although a previous study [8] discusses disadvantages of employing a pulsed laser system in oxygen GASMAS-settings, the pulsed dye-laser system was used here to study the temporal photon scattering inside the tissue of wild boar lungs, improving on the simple models used in the previous study.

3.4 Temporal Photon Scattering in Wild Boar Lung

Previous research about GASMAS lung monitoring has been focused on neonatal patient groups [1][5][6][7]. The first steps towards exploring GASMAS in larger geometries were taken by Lin et al. [8]. In their study, a pulsed dye-laser system was successful in assessing the temporal light scattering in pieces of styrofoam. The styrofoam pieces were up to 60 cm thick. Because styrofoam is a commonly used test-material for GASMAS measurements, the next natural step was to replace the styrofoam by biological samples. However, when introducing simple tissue models like chicken and pork, the temporal scattering could no longer be properly assessed. It was then speculated that the next step should be to test the same measurements on gas-inflated lung tissue.

Therefore, a similar pulsed dye-laser system was now used in this degree project for measurements on wild boar lung. The purpose was to study the temporal scattering inside lung tissue in a GASMAS-setting, which had not been done before. The experimental set-up and the measurements are presented below.

3.4.1 Pulsed Dye-Laser Instrumentation for Lung Measurements

The pulsed laser-system is schematically displayed in Figure 14. The output wavelength at 760 nm was produced by a dye-laser (PRSC-D-18, Sirah), which was pumped by the second harmonic output at 532 nm of a pulsed Nd:YAG laser (PRO 290 - 10, Spectra Physics). The pulse-durations were in the range of $6 - 8$ ns, emitted with a frequency of about 10 Hz. This resulted in pulse peak-powers in the MW-range. The 760 nm light was directed onto the target sample. Behind the sample volume, the light was measured with a photo-multiplier tube (H10721-20-01, Hamamatsu). The signal was read in an oscilloscope (Waverunner 6100, LeCroy).
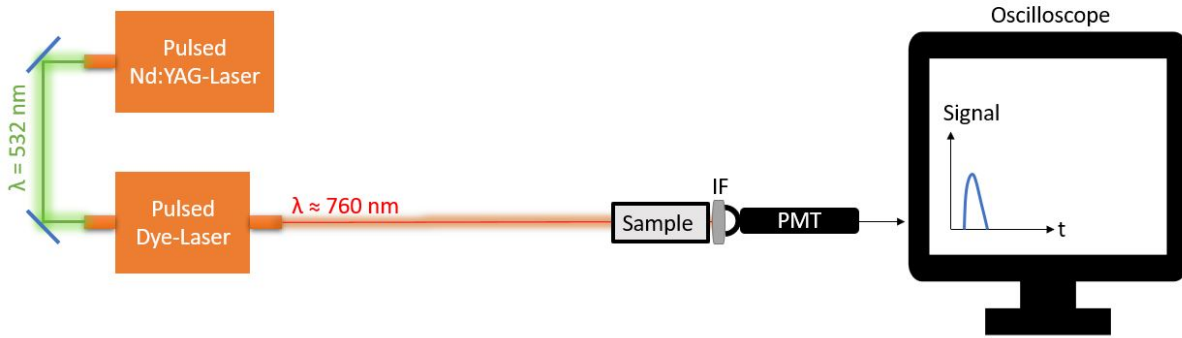
Figure 14: Schematic illustration adapted from [8] of a pulsed laser-system used for GAs in Scattering Media Absorption Spectroscopy (GASMAS) measurements. A dye-laser was pumped by the second harmonic out-put at 532 nm from a pulsed Nd:YAG laser. The dye-laser output wavelength was 760 nm. The light entered the sample volume and was then detected with a photo-multiplier tube (PMT) equipped with an interference filter (IF). The signal was displayed with an oscilloscope.

3.4.2 Procedure of Lung Measurements with Pulsed Light

The laser light from the TiSa-laser impinged on the lung tissue from two lungs of wild boar. Each lung was about 21 cm $\times$ 9 cm $\times$ 6 cm. This can be compared to a typical chest diameter of $6 - 10$ cm for that of a newborn preterm infant weighing about one kilogram [5]. The boar lungs could be supplied with air and/or nitrogen gas via an endotracheal tube and a bag valve mask. Behind the lungs, the photo-multiplier-tube measured the transmitted light. Because the laser-pulses could be scattered and reflected on the surfaces of the ambient room, it was important to prevent the room-scattered light from reaching the detector. To this end, the lungs were submerged in a dark box encapsulated with aluminium foil and dark shields, with the purpose to block out any light from the room. Moreover, an interference-filter (FB760-10, Thorlabs) permeable to 760 nm $\pm$10 nm was placed before the detector.

In order to investigate light attenuation due to scattering, the laser wavelength was first chosen so that it did not coincide to an absorption line of oxygen. This wavelength is referred to as an off-line wavelength (760.878 nm), which was very close to that of an absorbing wavelength. Then, the wavelength was switched to an on-line (760.9449 nm) absorbing one. The measured light intensity was studied as a function of time for both types of wavelengths. By dividing the signal obtained with the on-line wavelength to that of the off-line, the absorption can be indicated. If there is absorption, this on/off-line ratio is expected to have a downwards slope. A downwards slope means that the difference in arrival of the on-line and the off-line light to the detector increases for late-arriving photons. This can be interpreted as a sign of absorption because late-arriving photons can be assumed to have scattered a long path length inside the lung tissue, whereby the possibility of absorption of the on-line light is also increased. This way, a steeper downwards slope corresponds to increased absorption.

Furthermore, to be able to study the light scattering due to the presence of lung tissue in the measured signal, a measurement of the laser-pulse profile itself had to be taken for comparison. This was done with the off-line wavelength with the lung-sample removed.

Using the same pulsed-laser set-up as above, measurements were also made on styrofoam by replacing the lungs with a piece of styrofoam. Measuring with a pulsed dye-laser system on styrofoam has been done successfully before [8], and it was repeated now for comparison.

The set-up from the lung measurements is presented in a summarising overview in Figure 15.
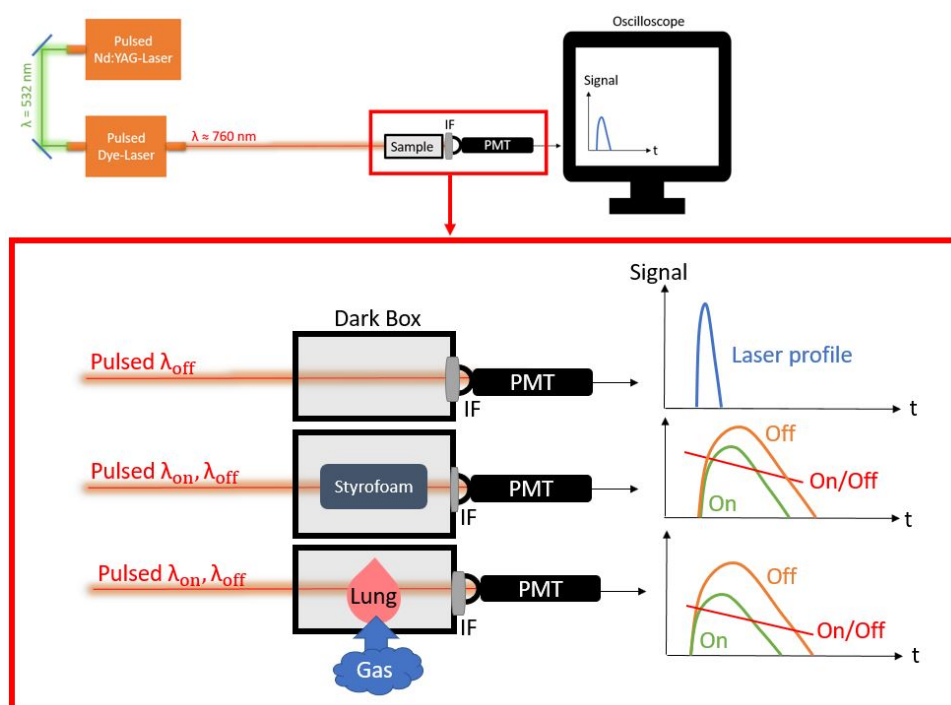

Figure 15: Experimental set-up with a pulsed dye-laser to measure on a lung sample (bottom), a piece of styrofoam (middle) and to measure the laser profile (top). The three set-ups in the red box are part of a greater laser-system consisting of a pulsed Nd:YAG-laser and a dye-laser for absorption spectroscopy (see Figure 14). In the top set-up, the wavelength is tuned to an off-line value, corresponding to low oxygen gas absorption, and then directed to an empty dark box of air before reaching a photo-multiplier tube (PMT) equipped with an interference filter (IF). This results in a laser-profile signal. In the bottom set-up, measurements are done on wild-boar lungs inside the dark box. The lungs could be gas-supplied and measurements were done with off-line and on-line wavelengths, where the on-line wavelength corresponds to oxygen gas absorption. This results in an off and an on signal, whereby the absorption corresponding to the ratio between the two signals can be studied.

3.4.3 GASMAS-Signals Using Pulsed Light

Styrofoam and Lung Measurements with 2 mJ Pulse Energy

Test-measurements on styrofoam are presented in Figure 16a, where also the laser-profile is shown for comparison, as well as the ratio of the on/off signals. Measurements through lungs with air-supply are presented in the same way in Figure 16b. To study the temporal scattering, normalised curves of the off-signals are displayed in Figure 17a, with a zoom-in on the lung-measurements in Figure 17b.
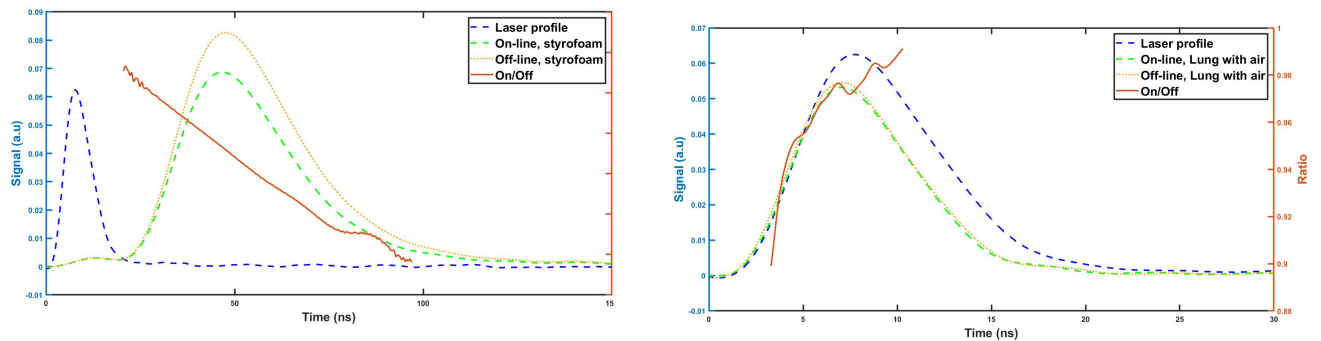
(a) Measurements on styrofoam with dimensions 21 cm × 9 cm × 6 cm.

(b) Measurements on wild boar lungs with air-supply.

Figure 16: Measurements with a dye-laser sending out pulses about 10 ns long with pulse-energies of $1 - 2$ mJ. The laser-profile, on-line and off-line signals are indicated (dashed). The red curve (whole-drawn) is the ratio of the green on-line curve divided by the yellow off-line curve. The signal amplitude is measured in arbitrary units. In each plot, the on-line and off-line curves are plotted in the same vertical scale whereas the laser-profile has a different scale.
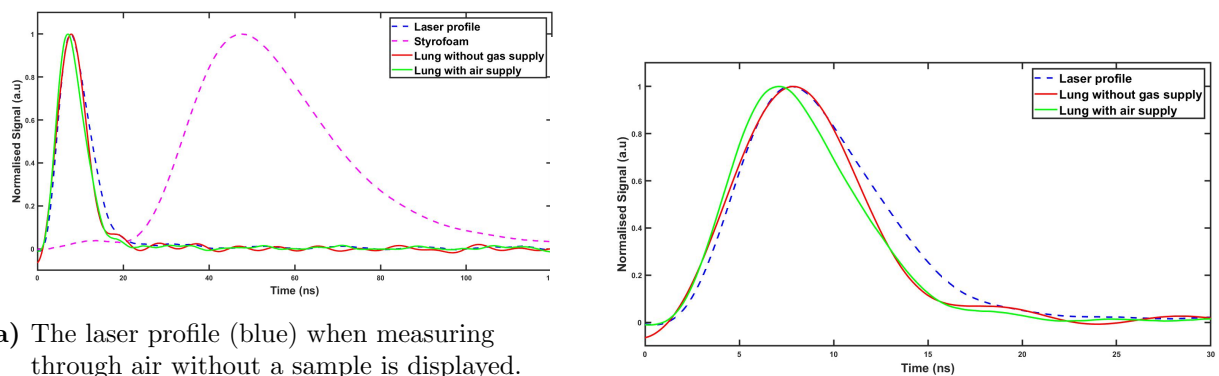
(a) The laser profile (blue) when measuring through air without a sample is displayed. Measurements were done on styrofoam (pink) and lungs with (green) and without (red) air-supply. For better presentation of the lung-measurements, the same graphs are presented in Figure 17b in a different horizontal scale.

(b) Measurements on lung tissue compared with the laser-profile are presented. The same information is visible in (same info as Figure 17a), however on a different vertical scale.

Figure 17: Normalised off-line signals from measurements with a pulsed dye-laser, with pulses about 10 ns long and with energies of about $1 - 2$ mJ. The off-line wavelength is chosen so that is does not correspond to oxygen gas absorption.

In Figure 16a where the styrofoam measurements are presented, the red on/off-curve shows a downwards slope, indicating absorption. Moreover, the delay of the on- and off-line signals compared to the laser-profile confirms that styrofoam is a strongly scattering media. Compared to styrofoam, the lung measurement in Figure 16b does not show a similar on/off-ratio, nor is there a delay or broadening of the on- and off-curves compared to the laser profile. This indicates that the delay of photons in the lung tissue due to scattering is small compared to the laser pulse duration.

Normalised off-line curves that are presented in Figure 17a indicate that there is a difference in light detector-arrival time between using lung tissue or styrofoam as sample. Compared to the laser-profile, the styrofoam signal shows a clear delay and broadening. The lung-signals are more difficult to interpret, why they are presented again in Figure 17b, but with increased horizontal resolution. Here, in Figure 17b no broadening nor delay is seen for the lung-signals compared to the laser-profile. The reason that the lung curves are a little delayed behind the laser-profile in Figure 17b could be due to some uncertainty in the trigger to the oscilloscope.

This indicates that the pulsed laser method cannot be used to study the temporal scattering nor the absorption at 760 nm in lungs, if a pulse-energy of $1 - 2$ mJ is used. Next, the pulse-energy was increased to 40 mJ, hoping to better probe the temporal scattering and absorption within lungs.

Lung Measurements with 40 mJ Pulse Energy

Similar lung measurements were done as before, but now with 40 mJ pulse-energy. Moreover, nitrogen gas was also flushed into the lung tissue. Measurements on lungs with air Figure 18a or nitrogen gas Figure 18b supply are presened in Figure 18. The ratios from Figure 18a and Figure 18b are presented again in Figure 19b (40 mJ pulse-energy), together with the styrofoam slope in Figure 16a ($1 - 2$ mJ pulse-energy). The corresponding normalised off-line curves are shown in Figure 19a.
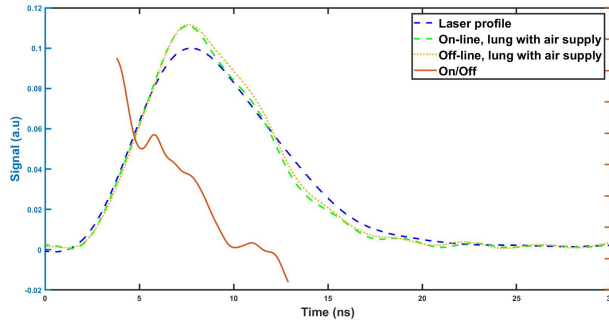
**(a)** Signals from air-supplied wild boar lungs.
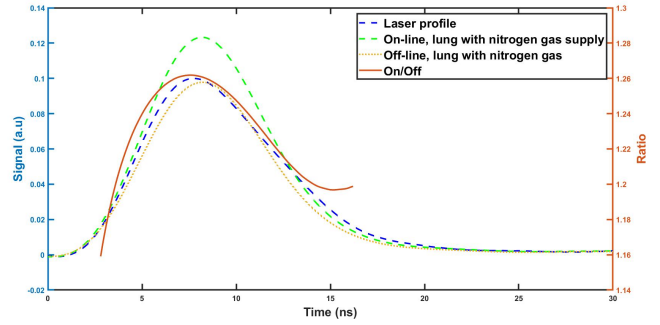
(b) Measurement from wild boar lungs that were supplied with nitrogen gas.

Figure 18: Pulsed dye-laser measurements on wild boar lung, with pulses about 10 ns long with pulse-energies of 40 mJ. The on-line and off-line signals are preseted alongside the laser-profile (dashed). The ratio (whole-drawn) of the on-line divided by the off-line curve is also shown. The units of the vertical signal amplitudes are arbitrary. The on- and off-line curves in each plot are plotted in the same vertical scale, but the laser-profile in a different scale.
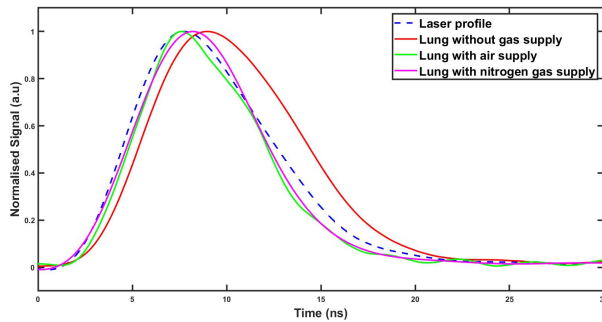
**(a)** Normalised off-line signals from pulsed dye-laser measurements. The pulses were about 10 ns long.
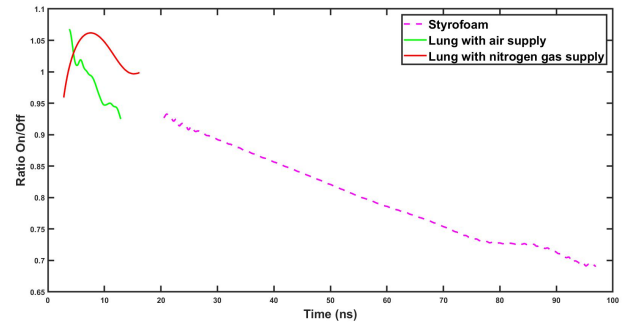
(b) On/off-ratio curves from measurements with a pulsed dye-laser. The on-wavelength corresponded to oxygen gas absorption whereas the off-wavelength did not. Both wavelengths were however very close. A ratio-curve with a downwards-slope indicates oxygen gas absorption in the sample. The samples investigated were styrofoam $(1-2$ mJ pulse-energy) and gas-supplied lung tissue (40 mJ pulse-energy). The lung on/off-signals are the same as are presented in Figure 18, but presented again here for comparison with the styrofoam on/off curve from Figure 16a.

Figure 19: Normalised curves and on/off-ratio from pulsed dye-laser measurements on wild boar lungs. The pulse-energy was about 40 mJ.

In Figure 18a, the red downwards slope indicates oxygen absorption in the lungs. The same slope is not seen for nitrogen gas in Figure 18b, as was expected. The temporal scattering in Figure 19a does not indicate heavy sacttering of light inside the tissue.

The absorption slope-curves in Figure 19b suggest that the system was able to detect styrofoam light scattering better than scattering in lungs.

The lung measurements with air-supply that are shown in Figure 18 and Figure 19 correspond to the best air-supply measurements on lungs that were taken. Even with the best air-supply results, it was not possible to see the scattering inside the lungs (see Figure 19a). Below is presented one air-supply (Figure 20a) and one nitrogen gas-supply (Figure 20b) measurement with 40 J pulse-energy, which were not as expected. It is difficult to intepret Figure 20. The air-measurement in Figure 20a was expected to show a downwards red slope, whereas the nitrogen gas red ratio-curve in Figure 20b was expected to lack clear a slope-trend. It is speculated that something has gone wrong in Figure 20b; the difference between the on- and the off-curves is expected to be small. These measurements indicate that the pulsed dye laser-system is not always able to investigate the temporal light scattering inside lung tissue nor oxygen gas absorption.
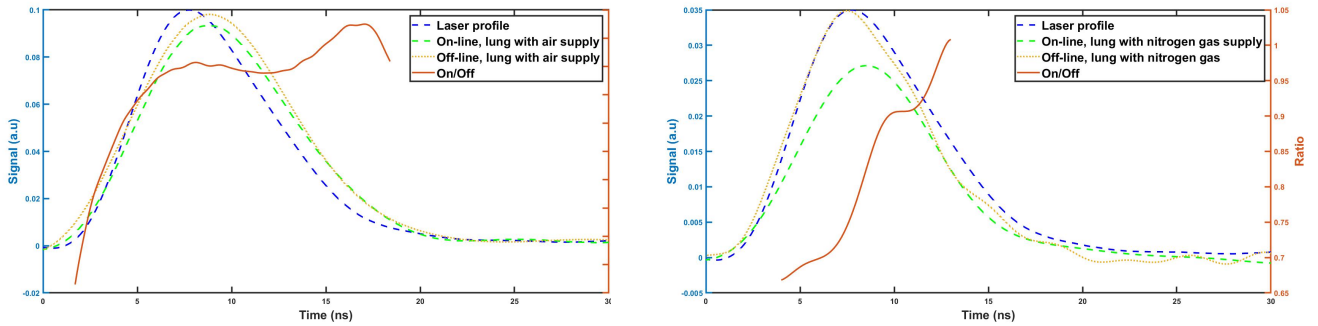
(a) Signals from air-inflated lungs.

(b) Measurements on nitrogen gas supplied lungs.

Figure 20: Less successful dye-laser spectroscopic measurements in gas-supplied wild boar lungs, with an on-line wavelength corresponding to oxygen gas absorption. The close-lying off-line wavelength does not correspond to oxygen gas absorption. The pulse energies were about 40 mJ, and the pulses were about 10 ns long.

3.4.4 Evaluation of Pulsed GASMAS Signals

Altogether, the quality of the measurements on lungs with the pulsed dye-laser system vary. There was no fully successful way of studying the temporal scattering inside lung tissue nor the absorption with this system. Attaining high light powers for oxygen GASMAS in lung tissue with a pulsed dye-laser system is probably not ideal. This has also been indicated by Lin et al. [8], and was now proved in a more realistic wild boar lung.

The main problem why the pulsed laser system could not asses temporal scattering in wild boar lungs is probably that the scattering in lung tissue is too low, resulting in a too low temporal delay from scattering compared to the laser-pulse duration. Using shorter laser pulses might enable better assessment of the scattering inside lung tissue, however at the cost of reduced wavelength-precision. All the same, these high-energy pulsed measurements demonstrate good light transmission through the large lungs, suggesting that higher powers can penetrate through large tissue volumes.

From these pulsed GASMAS measurements, exploring how to amplify the laser light power of a diode-laser system with an OTPA becomes even more relevant. The upcoming chapter discusses how to incorporate an OTPA into the previously discussed diode-laser system.

4 Towards Higher Powers

The purpose of introducing an OTPA into a diode-laser system was to amplify the power of the laser light, with the goal to approach oxygen GASMAS lung measurements in large geometries. Using an OTPA was suggested by previous research [8], because it could allow the basis of the present functioning GASMAS-systems to be kept intact, preserving the beneficial WMS and lock-in techniques for signal enhancement.

This chapter presents the attempts of incorporating an OTPA into the previously used diode-laser system (illustrated in Figure 9). A critical aspect for obtaining optimal amplification is that the seed-laser impinges on the input facet of the OTPA in an ideal way [18]. Such ideal impingement requires ideal alignment and beam focusing, topics which relate to optics and diffraction limit considerations. Therefore, optics and diffraction limit analyses are also presented.

Diffraction limit computations investigate how well it is possible to focus a laser-beam. Because this depends on the laser beam's cross section intensity profile and the beam diameter, the beam diameters is also investigated.

The efforts of incorporating the OPTA into the diodlaser system do not show ideal amplification of the laser light. Possible ways of improving the system for future work are presented.

4.1 OTPA Setup and Theoretical Diffraction Limit

The amplifying component of an OTPA is a crystal. In order for the tapered amplifier to achieve optimal amplification, the seed-laser must impinge on the input-facet of the crystal with an angle and position close to ideal. The basic alignment idea inspired by application notes [18] from the laser and OTPA company, toptica Eagleyard, is now presented: the diode seed-laser with diameter D, which is in the mm-range, is directed towards an aspherical lens. The lens has a focal length f and focuses the beam onto the μm input-aperture of the OTPA. The OTPA has a single-mode channel and a tapered region. Thereafter the beam exits through the output aperture of hundreds of μm and diverges. A schematic overview of the alignment idea is presented in Figure 21.
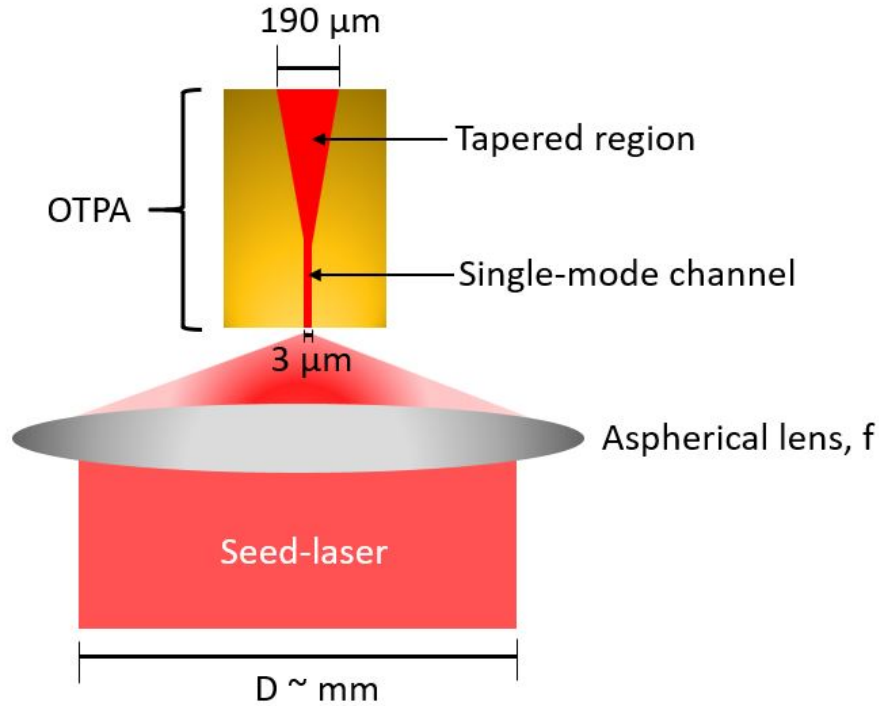
Figure 21: Injecting an optical tapered amplifier (OTPA) with a seed-laser, by focusing the beam onto the 3 μm input-aperture with an aspherical lens. The light first enters a single-mode channel, then a tapered region.

In this project, the amplifying crystal of the OTPA (EYP-TPA-0765-01500-3006-CMT03-0000, Toptica Eagleyard) was fitted in a metal housing. The input and output apertures of the crystal were 3 μm and 190 μm respectively. Via the metal housing, the crystal was supplied with a current in order to obtain population inversion. The current was supplied from a laser-driver device, Combosource (6340 Series ComboSource, Arroyo Instruments). The Combosource also controlled the temperature of a TEC mount (285-01 TECMount, Arroyo Instruments) upon which the OTPA metal housing was mounted. Both the current supplied to the crystal and the temperature control of the TEC-mount were thus controlled by the Combosource device. The output-plane of the OTPA-setup is schematically illustrated and photographed in Figure 22.
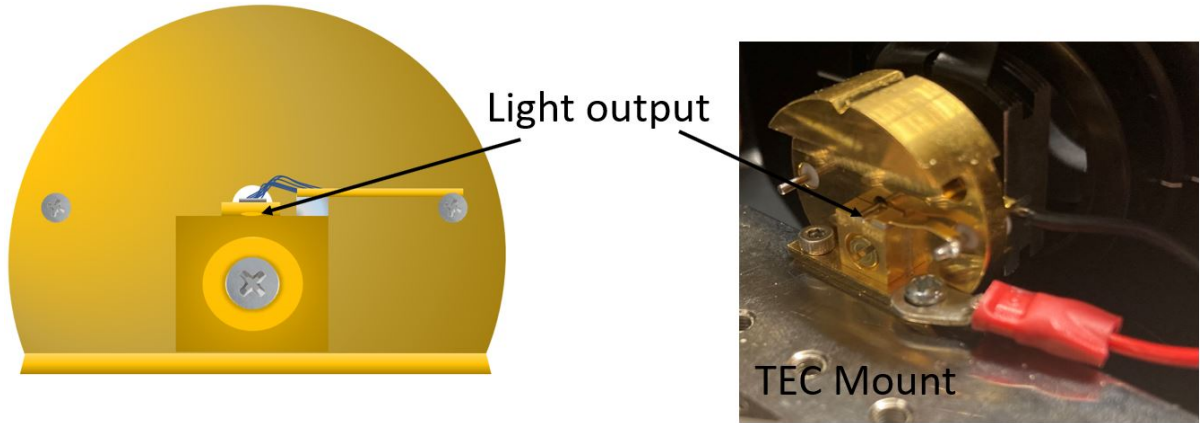
34

Figure 22: The output front plane of an otpical taprered amplifier (OTPA) that is fitted into a metal housing. The metal-housing is mounted upon a TEC temperature-controlling mount. The cables emerging from the metal-housing delivers a current supply that is essential for amplification.

Before assembling the OTPA into the diode-laser system, it was important to consider the width D of the seed-laser beam and the focal length f of the lens. Given that the OTPA input aperture is about 3 μm, the lens had to focus the beam so that the focus-diameter was also in the μm-range. This required basic theoretical considerations about diffraction limits and beam divergence.

4.1.1 Theoretical Diffraction Limit Considerations

In the cross-section of a gaussian beam, the highest intensity is located in the center, while the intensity gradually decreases in the outwards direction. Consider the situation depicted in Figure 23: if a gaussian collimated beam of diameter D is incident on a lens with focal-length f, the focus-point diameter, d, is given by Equation 2 ([19] p. 80 - 94).

$$\begin{cases} d = \frac{4}{\pi}\lambda F \\ F = \frac{f}{D} \end{cases} \tag{2}$$

where λ is the wavelength. To explore if it was possible to reach a μm-size of the focus-point d, the laser profile was studied to get information about the beam diameter D.
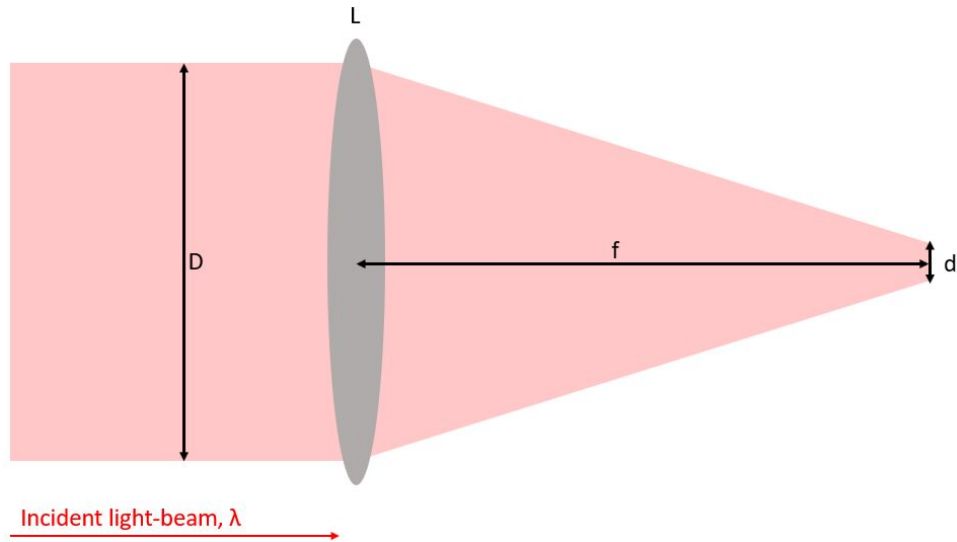
Figure 23: A collimated light-beam of wavelength λ and diameter D is incident on a lens L with focal length f. The focus point diameter is d.

Because a Gaussian beam diameter increases after propagating long distances, it was relevant to investigate the beam diameter for increasing distance from the laser output. The beam diameter D was defined as $D = 2\text{FWHM}/\sqrt{2\ln(2)}$, where FWHM is the *Full Width at Half Maximum* of a Gaussian curve [19].

4.2 Beam Profile of the Diode-Laser

In order to investigate the beam profile, a camera (UI-3240CP-NIR-GL, iDS) and neutral density (ND) filters were used. The images of the beam cross-section are shown in Figure 24. Figure 24 shows that the cross section of the beam intensity profiles are close to gaussian, even at distances longer than one meter from the laser-output (see Figure 24c and Figure 24d).
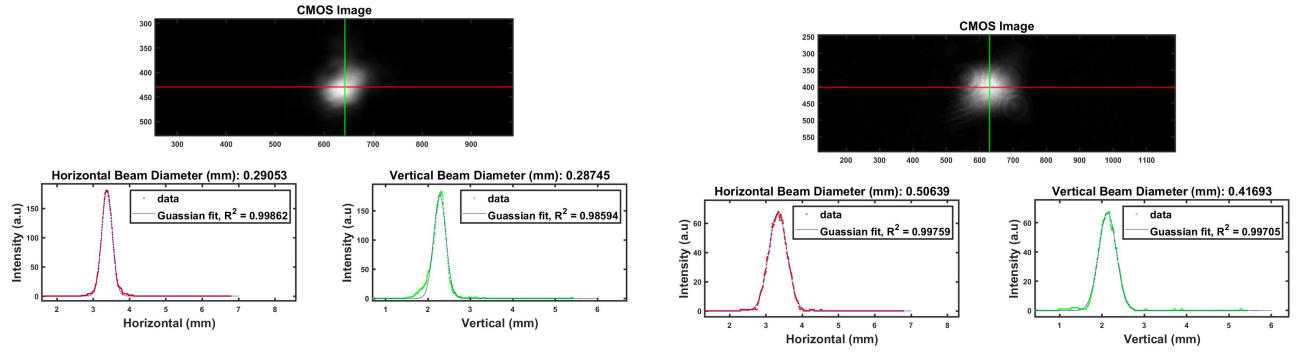
(a) Laser beam intensity cross-section 17 cm after laser-output aperture. The laser output laser light is attenuated with neutral density (ND) filters of optical density (OD) 8.1.

(b) Intensity cross section of a laser beam 50 cm after laser output-aperture, with neutral density (ND) filters with optical density (OD) 1.8.
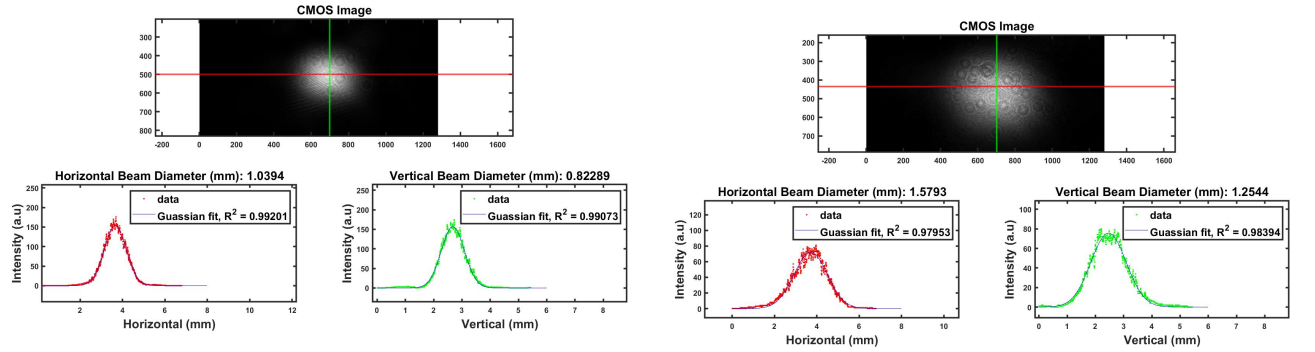
(c) Cross section of the laser beam intensity at 113 cm after the laser output aperture. Neutral density (ND) filters with optical density (OD) 7.1 were applied.

(d) Laser beam intensity cross-section 175 cm after laser-output aperture. Neutral density (ND) filters with optical density (OD) of 7.1 were applied.

Figure 24: Images of a diode-laser beam profile, taken with a Complementary Metal Oxide Semiconductor (CMOS) camera at different distances from the laser-output. In each subfigure, the top image displays the CMOS-image while the bottoms two plots show the intensity distribution in the vertical (green) and horizontal (red) directions. The goodness-of-fit, R^2, is also displayed to indicate how well the intensity data fits a Guassian. The distance from the laser-output to the CMOS-camera is indicated below each subfigure.

From the beam profiles presented in Figure 24, the diameters are computed as $D = \text{FWHM}/\sqrt{2\ln(2)}$ where FWHM is based on the gaussian fit. Taking the mean of the vertical and horisontal beam diameters for the distances 17 cm, 50 cm, 113 cm and 175 cm results in approximate mean diameters of 1.44 mm, 0.93 mm, 0.46 mm and 0.29 mm respectively.

Apart from D, the lens foal length f must also be considered. It is noted that short focal-length f is favourable because it decreases d (see Equation 2). However, very short focal-lengths make the alignment more difficult. A lens with $f = 11$ mm was chosen as a trade off between ease of alignment and wanting a short f for diffraction limit purposes.

Plugging the approximate mean diameters as D into the formula in Equation 2, together

with $\lambda = 760$ nm and $f = 11$ mm, gives the focus-diameters as shown in Equation 3.

$$d = \frac{4}{\pi} \cdot 760 \cdot 10^{-9} \cdot \frac{11 \cdot 10^{-3}}{D} \approx \begin{cases} 7.4 \ \mu\text{m}, D = 1.44 \text{ mm} \\ 11.4 \ \mu\text{m}, D = 0.46 \text{ mm} \\ 23.1 \ \mu\text{m}, D = 0.93 \text{ mm} \\ 36.7 \ \mu\text{m}, D = 0.29 \text{ mm} \end{cases} \tag{3}$$

It is possible to to have a small focus-point within the gain-volume of the OTPA-crystal if D is large, as seen in Equation 2. Equation 3 shows that it is possible reach μm-wide focus size if the laser has a large input diameter. A large diode-laser beam diameter can be attained if the beam travels long distances in air. With this information, it was reasonable to set up and try to align the system according to Figure 21.

## 4.3 Aligning the OTPA into the Diode-Laser System

Based on the alignment idea in Figure 21, the OPTA was set-up in the diode-laser system as shown in Figure 25. The collimated laser light was directed onto an optical isolator (IOT-5-780-VLP, Thorlabs). The optical isolator transmits light only in the forwards direction, with the purpose to protect the laser from potential high-energy back-reflected light. After the isolator, the light was directed with two mirrors, $M1$ and $M2$, onto a lens (A397TM-B, Thorlabs) with $f = 11$ mm. The optical axis was defined by introducing two irises, $I1$ and $I2$, between the mirrors. The lens was mounted on a translation stage allowing for mm adjustment in the x-, y- and z-direction. The light entered the input rear facet of the crystal, whereafter it diverged on the output front side. The power of the diverging light was measured with a power-meter (S302C, Thorlabs) and also directed with a prism onto a microscope objective (PLN 4X, Olympus). Via the microscope objective and a camera (CM3-U3-13S2M-CS, Edmund Photonics), the light at the out-put front facet of the OTPA was imaged. The image was displayed in a Beam Profiler software developed by Anders Persson, reasearch engineer at the Division of Atomic Physics, Lund University. The software was used for feedback when aligning the system, so that as much light as possible was focused with the lens onto the gain volume of the amplifier. The distance that the light travelled from the optical isolator to the lens is about 113 cm.

The alignment was done according to these steps, with the goal to amplify the laser light that impinges on the OTPA:

1. The laser was switched off, keeping only the OTPA switched on. The driver-current was set to 1600 mA, which was close to the upper limit of the recommended settings. The ASE was then used to align the lens and $M1$, so that the light from the ASE in the backwards direction passed in a collimated way through both irises. With this step, an optical axis was defined.

2. The next step was to align the laser onto this optical axis, ensuring that the laser impinged on the gain-volume of the OTPA crystal. This was done by switching off

the OTPA and switching the laser on. Now, $M2$ was adjusted so that the laser-light travelled through both irises and towards the lens. In this step, the laser light path was assumed to overlap with the ASE-path.

3. Next, the beam profiler screen was studied, alternating in switching either the laser or the OTPA on. The mirrors and lens were adjusted so that the light-ouput area, whilst keeping only the OTPA switched on, overlapped with the light-ouput area of the laser.

4. Finally, both the OTPA and laser were switched on. The lens and mirrors were again adjusted until an intensity increase could be visible by the beam profiler image and the power-meter, demonstrating that amplification was achieved even though the overlap and axis alignment was not optimised.
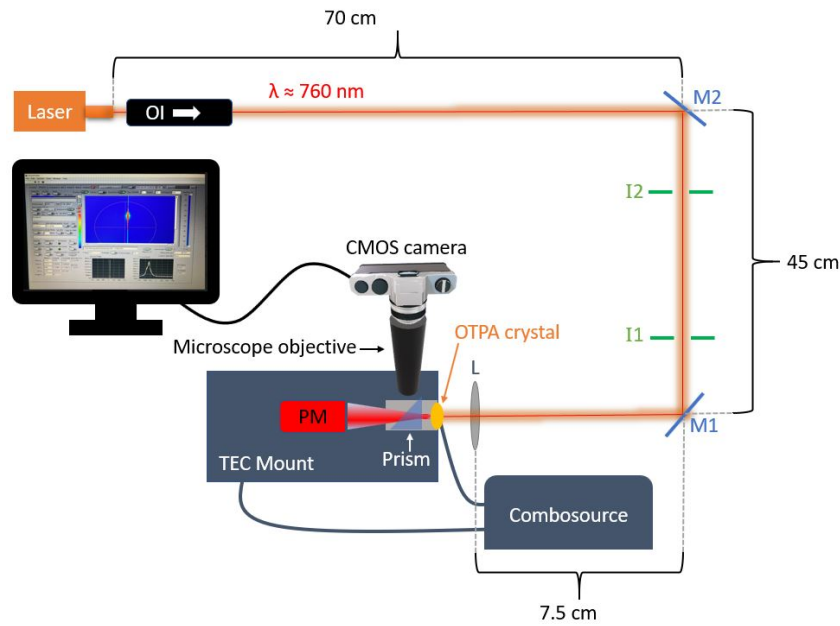
(a) Schematic illustration.
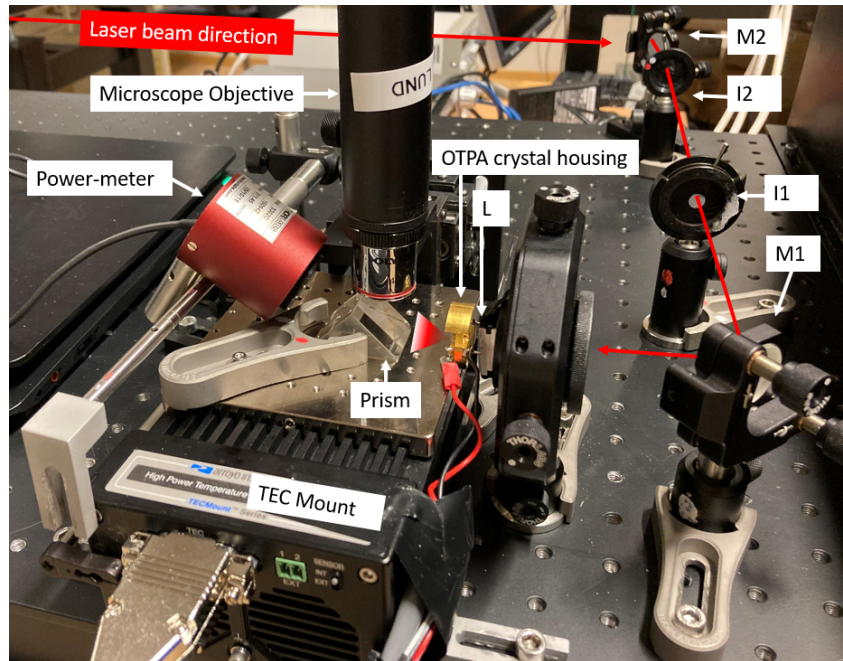
(b) Annotated photography.

Figure 25: Set-up to seed a diode-laser into an optical tapered amplifier (OTPA) crystal for light power amplification. The OTPA amplifying crystal is mounted on a TEC mount. A Combosource instrument controls the temperature of the TEC mount and the current supply to the crystal. Collimated laser light with a wavelength of about 760 nm enters an optical isolator (OI) and is then directed with the help of two mirrors, $M1$ and $M2$, onto a lens, L. The optical isoolator is about 10 cm long, making the distance from the OI output to L about 113 cm. Two irises, $I1$ and $I2$, are used to define the optical axis between the mirrors. The lens then focuses the light onto the input rear facet of the OTPA crystal, after which the light diverges and the light power is measured with a power-meter (PM). A prism directs part of the diverging light towards a microscope objective, so that the out-put front facet of the OTPA is captured by a Complementary Metal Oxide Semiconductor (CMOS) camera. The light intensity profile of the out-put light, captured by the CMOS camera, is displayed on a screen in a Beam-Profiler software developed by Anders Persson. Persson is a research engineer at the Division of Atomic Physics at Lund University.

4.3.1 Indications of a Small OTPA Amplification

The shadowed outline of the output facet of the OTPA as imaged by the Beam-Profiler software is presented in Figure 26.

Figure 26: The output facet of an Optical Tapered Amplifier (OTPA), imaged with a microscope objective (PLN 4X, Olympus) via a Beam-Profiler software developed by Anders Persson, research engineer at the Division of Atomic Physics at Lund University.

The powers measured behind the prism are presented in Table 2 in Appendix B. It is noted here that the measured power behind the OTPA reflects only the light that is reflected onto the power-meter by the prism (compare with photography in Figure 25). The powers in Table 2 are plotted in Figure 27. Complementary to this, the graphic feedback from the beam-profiler software is displayed in Figure 28.
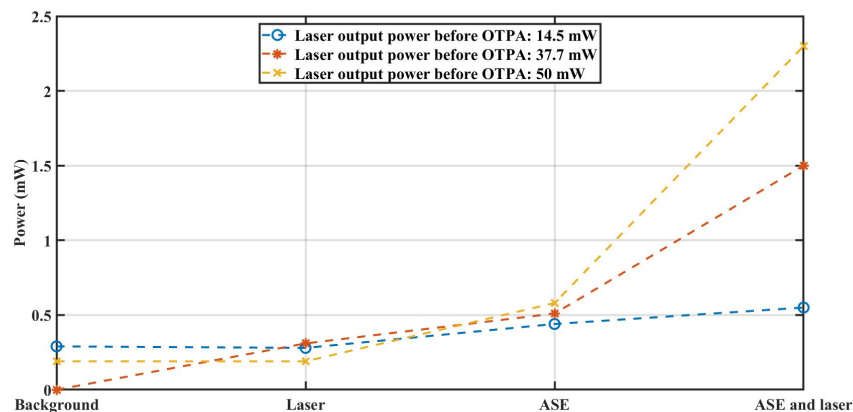
Figure 27: The power collected via a prism at the out-put face of an Optical Tapered Amplifier (OTPA). From the left, the background measurement is shown first, where neither OTPA nor laser was on. The following measurements correspond to first only the laser and then only the OTPA switched on. Lastly, the right-most measurement is the power after the OTPA, when both the laser and the OTPA are switched on. The measurements were done with laser output-powers before the OTPA ranging from about 15 - 50 mW, as indicated by the plot legend.

(a) Background

(b) Seed-laser

(c) Amplified Spontaneous Emission (ASE) from an Optical Tapered Amplifier (OTPA)

(d) Amplified Spontaneous Emission (ASE) from an Optical Tapered Amplifier (OTPA) and seed-laser light
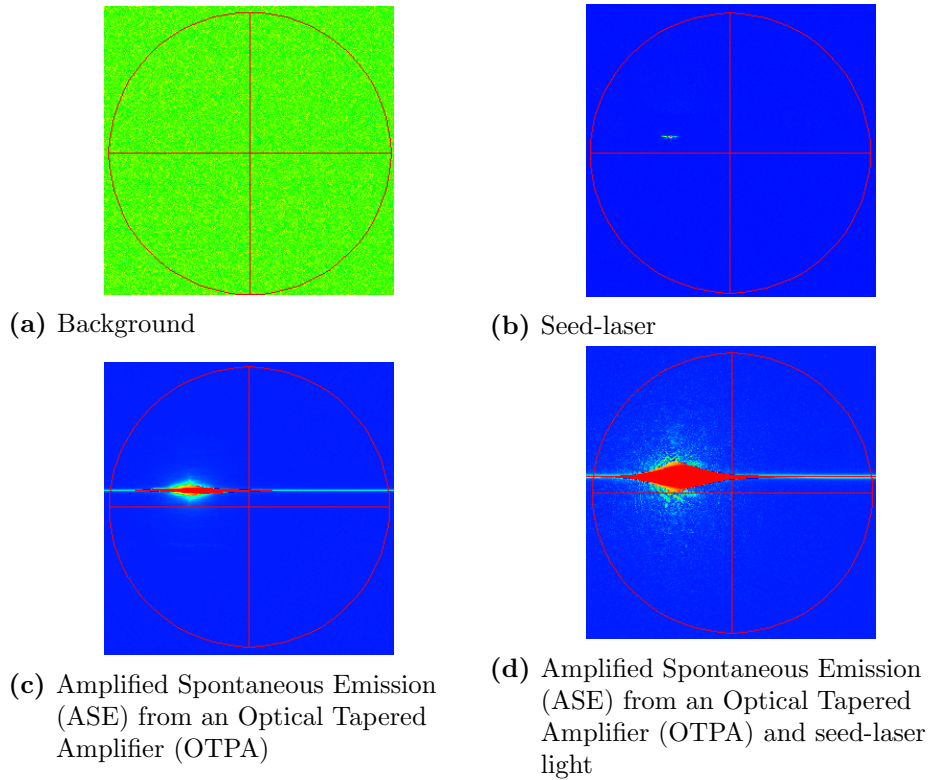
Figure 28: Photographs of a Beam-Profiler software screen are shown, which spatially indicates high intensity (red) or low (blue). The software is developed by Anders Persson, engineering researcher at the Division of Atomic Physics at Lund University.

The graphic intensity profiles and power trends in Figure 28 and Figure 27 indicate that there was indeed an amplification, albeit a small one. Figure 27 indicates that there is indeed some amplification of the light actually impinging on the gain-volume, if the incident laser light power is set to a high value. However, given the output powers of the laser (tens of milliwatts), the alignment is not optimal. Probably only a small fraction of the diode laser light passes through the OTPA crystal.

That the alignment is not optimal is also indicated by studying the spectrum of the light emerging behind the crystal. The spectra from the TPA and/or the seed-laser are presented in Figure 29. Because the green curve representing both the ASE and the laser has a clear narrow part in Figure 29b (higher laser power) but not in Figure 29a (lower laser power), it is indicated that the seed-laser amplification is enhanced by higher input-powers.
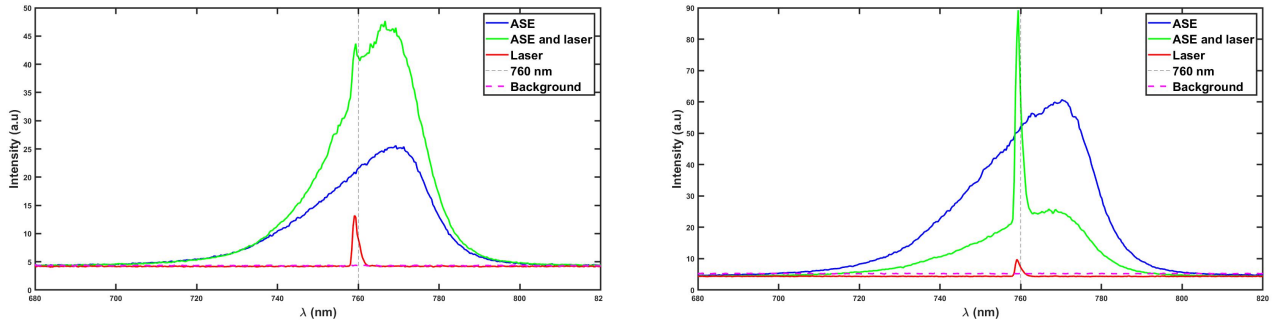
(a) The the seed-laser output power is about 15 mW. **(b)** The output power of the seed-laser is about 38 mW.

Figure 29: The spectra of Amplified Spontaneous Emission (ASE) of an Optical Tapered Amplifier (OTPA), the seed-laser and the background, for different seed laser powers. The intensities of the different curves are shown in separate arbitrary scales, making it irrelevant to compare intensity-differences.

4.4   Improving the OTPA-System

The purpose of this experiment was to try to incorporate an OTPA into the diode-laser system. Out of the laser light that actually impinged on the OTPA gain-volume, amplification was been seen. However, that was probably only a very small portion of the laser-light, making the amplification far from optimal. In order to improve the amplification, it is necessary that more of the input diode-laser light reaches the OTPA input-aperture.

In order to better focus the seed-laser onto the OTPA input facet, it is suggested to improve the mechanical adjustment of the crystal in relation to the optical axis of the laser. Now, only the lens allowed for translation in all three dimensions, but not the crystal itself. Having a high-precision xyz-transition stage for the crystal would enable more precise alignment.

Even if the OTPA would work optimally, it remains to investigate how the level of light detection in biological tissue is affected by light power. This is the topic of the next chapter.

5 Investigation of Light Transmission for Large Geometries

During this thesis work, the OTPA was not successfully incorporated into the diode-laser system. It was not possible to detect optimal amplification with the current setup, although improvements were suggested. The hope is that, if laser power amplification is achieved with an OTPA, oxygen GASMAS measurements in lung tissue can be made possible in larger geometries.

Now, measurements were done outside the scope of a diode-laser system, to find how tissue penetration depth is expected to vary with increasing laser power. To this end, a TiSa-laser was used that emitted CW light at 760 nm. The light wavelength could not be scanned fast enough to GASMAS measurements, but the light power could reach well up to 2 W. This made the TiSa-system appropriate for investigating 760 nm light penetration in tissue. As a model of scattering biological tissue, slabs of pork were used.

The results suggest that increasing the laser power increases the level of signal detection through model tissue slabs. This insight can be valuable as it inspires future work with trying to amplify the power of laser light, in order to achieve oxygen GASMAS measurements in lung tissue of large geometries.

5.1 Set-Up for Tissue Slab Measurements

The laser system used was a TiSa-laser system (SolsTiS EMM, M Squared). The TiSa-laser gain medium was pumped by the second harmonic at 532 nm of a Nd:YAG laser. The TiSa-laser beam was CW and its power could be tuned at least up to 2 W. Because no fast wavelength tuning was possible, the intensity of the laser-beam was modified instead by placing a fast-rotating chopper-wheel in the direction of the laser beam. The laser beam after the chopper wheel was directed towards slabs of pork. The pork was used as a simple model of scattering biological sample. The intensity was measured with a photo-diode (3590-08, Hamamatsu) equipped with an interference-filter (FB760-10, Thorlabs) with high transmission at 760 nm ± 10 nm. The detector was placed in close contact with the pork. The signal was displayed in an oscilloscope (Waverunner 6100, LeCroy).
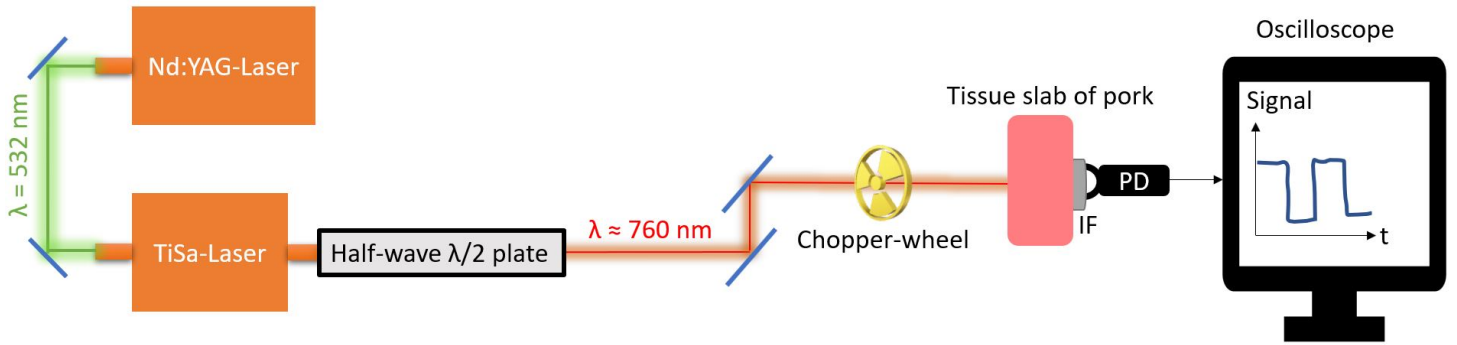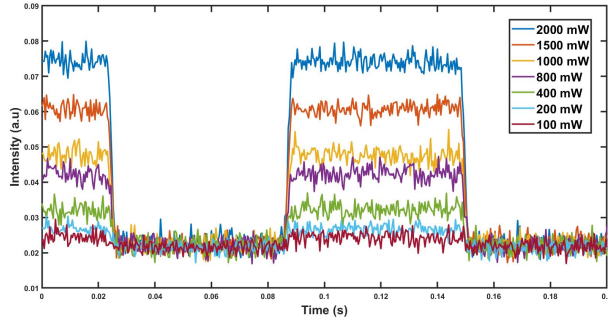
Figure 30: Set-up of a Titanium-Sapphire (TiSa) laser pumped by the second harmonic of a Nd:YAG-Laser. The power of the 760 nm TiSa-laser light can be tuned by rotating a half-wave plate. The light is directed with the help of two mirrors onto a chopper wheel, after which the light impinges on a tissue slab of pork. After the pork, a photo-detector (PD) equipped with an interference filter (IF) measures the transmitted light. The IF is permeable to 750 nm ±20 nm. The signal is displayed on an oscilloscope screen.

The laser-powers and slab thicknesses were gradually varied. For slab thicknesses equal to or thicker than 14 cm, the pork was covered in aluminium foil. The foil was used to block out unwanted light that might impinge on the detector, that had not travelled through the entire pork slab thickness. Moreover, averaging was applied to increase detection sensitivity.

5.2 Signal in Tissue for Varying Thickness and Power

Measurements were done on pork slabs of thickness from 7 cm - 17 cm, with powers ranging from 50 mW to 2000 mW. For tissue slabs of thickness 14 cm and thicker, the pork was covered in aluminium foil in order to make sure that the detected light has travelled through the pork thickness. This was relevant particularly for thicker tissue slabs, where it is expected to be more difficult to distinguish the signal above the noise. Example plots of several measurements with varying laser powers are presented in Figure 31, for 8 cm (Figure 31a) and 14 cm (Figure 31b). In Figure 31, the signals are assumed to reside where the intensities are highest, at the plateaus of the top-hat-like curves. The noise is assumed to reside in the depressions beside the top-hats. From a simple qualitative inspection, Figure 31 suggests that increasing the power makes it easier to distinguish the signal above the noise, especially for thicker tissue.

(a) Measurements on a pork slab 8 cm thick.
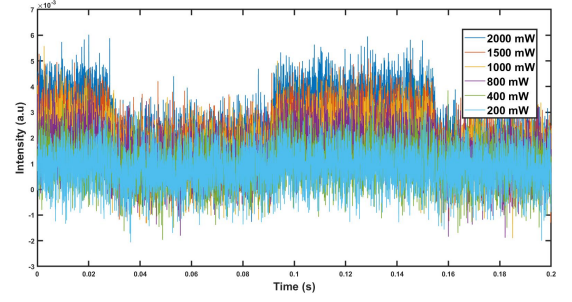
(b) Measurements through 14 cm thick pork slab covered in aluminium foil.

Figure 31: Measurements with a Titanium-Sapphire (TiSa) laser on pork slabs of varying thickness for varying laser powers.

In order to be able to quantitatively compare how well the signals can be distinguished above the noise, an SNR-value was introduced. The SNR-value was defined as the mean of the signal minus the mean of the noise, divided by the standard deviation of the noise. The SNR-deifition used is presented in Equation 4.

$$\text{SNR} = \frac{\text{mean of the signal - mean of the noise}}{\text{standard deviation of the noise}} \tag{4}$$

An example plot that marks the means of the signal and noise levels, measured through 8 cm of pork with light of 1 W, is presented in Figure 32. The SNR is also indicated.
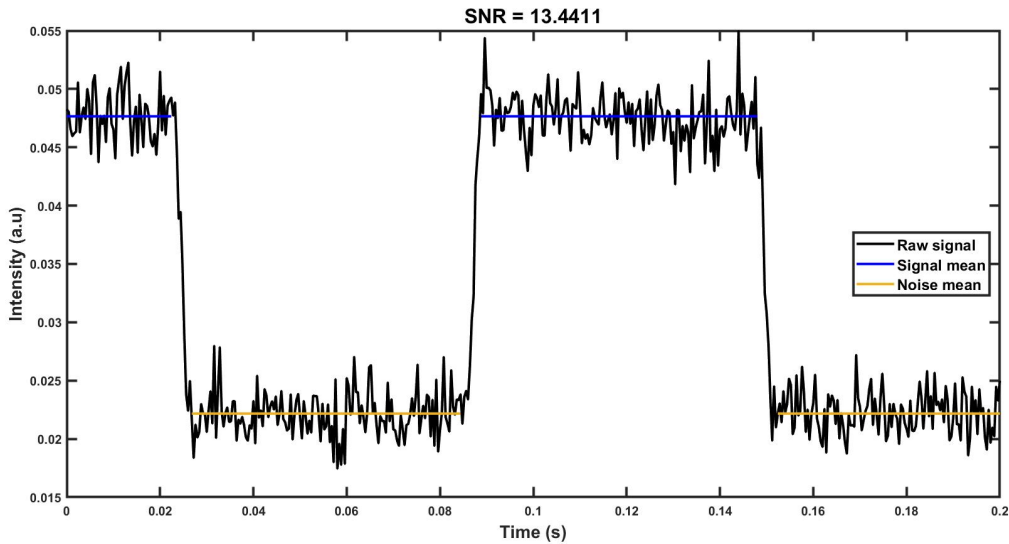

Figure 32: Signal intensity for a Titanium-Sapphire (TiSa) laser measurement through a pork slab of 8 cm thickness, with a laser power of 1 W. The means of the signal (blue) and of the noise (yellow) are indicated. A Signal-to-Noise-Ratio (SNR) is presented, as fund by taking the mean of the signal minus the mean of the noise, divided by the standard deviation of the noise.

The trend of the SNR-values for varying powers and tissue thicknesses are presented in Figure 33. It was expected that the SNR for measurements on a slab of a fixed thickness would increase with power, which overall agrees with Figure 33. Here, not all measurements are presented but the trend is representative for almost all measurements. The measurements through 11 cm - 13 cm of tissue were discarded because it is suspected that the measurements were not done correctly. The measurements through 12 cm rendered higher SNR values for all powers investigated than those of 11 cm. Measurements through 13 cm rendered higher SNR-values than all measurements through 10 cm - 12 cm. At these measurements for 11 cm - 13 cm, it is probable that light was measured at the detector that had not travelled through the entire pork thickness. This was probably not an issue for the thinnest slabs of 7 cm - 10 cm. This way, the measurements through 11 cm, 12 cm and 13 cm were discarded. Interestingly, the uphill SNR-trends seen in Figure 33 are broken slightly for the 10 cm measurement. The SNR-value for 2000 mW is about one below that at 1500 mW. Because the SNR-values are well above one for both 1500 mW and 2000 mW, this slight deviation from the trend is not considered to be important for the overall trend.
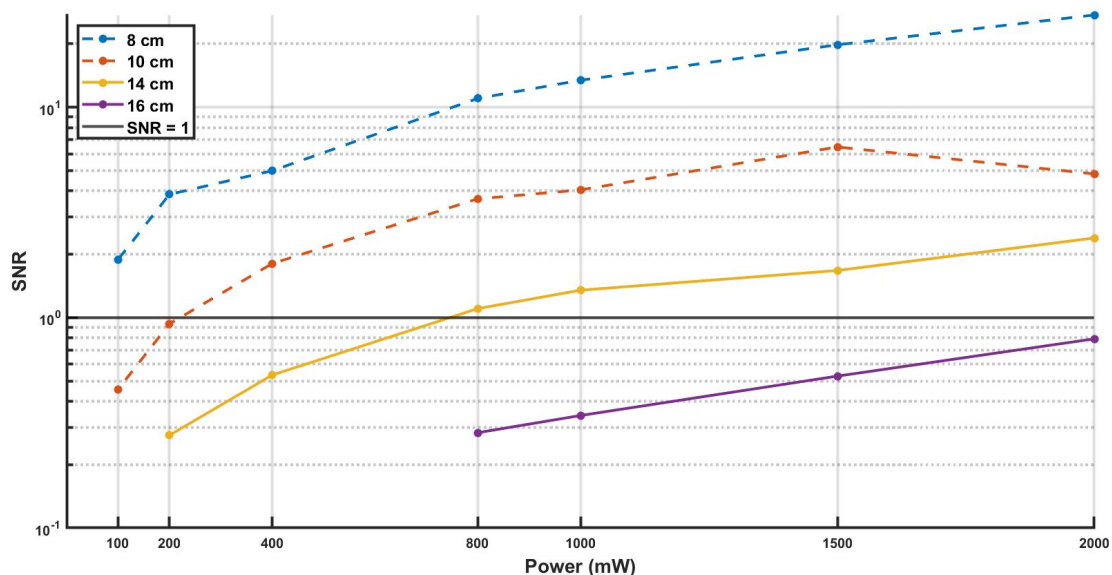
Figure 33: Signal-to-Noise-Ratio (SNR) from measurements with a Titanium-Sapphire (TiSa) laser on pork slabs of varying thickness.

Now it is assumed that laser light detection is possible through a tissue slab of a certain thickness if the SNR-value is above or equal to one. With this assumption, then Figure 33 shows that detection is possible through tissues of 8 cm, 10 cm and 14 cm with powers of at least 100 mW, 400 mW and 800 mW, respectively. To penetrate through 16 cm of tissue, then not even 2 W is enough. Not shown in Figure 33 is the measurement at 7 cm, where 50 mW was enough for light detection. Reaching from 7 cm to the double of 14 cm thus showed that the power had to be increased a factor of $800/50 = 16$, whereas only an increase of factor 4 was needed to go from 8 cm to 10 cm.

In relation to these findings, it is noted that the used OPTA can theoretically deliver powers up to about 1 W according to the specification [20]. This can be compared to the current method, where laser-powers below 50 mW were used with the diode-laser. Based on Figure 33, it would not even be reasonable to expect to to detect laser light after 10 cm of tissue at 50 mW whereas 1 W could allow up to 14 cm. In terms of physical lung geometries of a patient, it is indeed interesting to allow for scaling up from $\leq$ 10 cm to 14 cm light penetration. Of course it must be noted that the pork slabs used in this experiment is not a perfect model of the tissue fund in human. The intricacy of the tissue layers' optical properties found around the lungs can probably not be captured by pork slabs. However, the trend of light detection in Figure 33 is interesting. It is suggested that increasing the laser power indeed help to detect light through thicker tissue.

5.2.1 Higher Detection Limit with Increasing Power in Tissue

By studying how well 760 nm laser light can be distinguished above the noise level in biological tissue slabs, it is indicated that higher powers probably enables light to penetrate through longer distances in biological tissue. This encourages future work in trying to amplify the diode-laser light with an OTPA for GASMAS purposes.

6 Summary and Conclusion

In this project, experiments have been done to investigate how the current GASMAS technique can be scaled up to allow oxygen GASMAS in larger geometries.

First, a GASMAS-system was assembled based on a tunable CW diode-laser. This system was used for measurements on wild boar lungs. The measurements indicate that the present GASMAS-system is successful in performing oxygen GASMAS measurements in lung tissue, with about 26 mW through $3 - 5$ cm of tissue. However, this diode-laser system is limited in terms of power. Only powers up to 50 mW can be reached with this system. Moreover, a high-energy pulsed laser system was employed to try to asses the temporal scattering in lung tissue. However, there was no temporal delay due to scattering between measurements through lung tissue compared to the laser pulse itself. Downhill clear absorption on/off-curves were visible in far from all lung measurements with air-supply. This indicates that the CW diode-laser is preferred over the pulsed.

Second, attempts were made to incorporate an optical amplifier into the diode-laser system for power amplification. It is probable that a small amplification of the light impinging on the gain volume takes place, however the amplification is far from ideal. The critical aspect for successful amplification is likely that the input-facet of the OPTA and the seed diode-laser must be perfectly aligned. This was not achieved now, but might be if the system is upgraded with better alignment mounts.

Lastly, a high-energy TiSa-laser system was used to study light detection through tissue slabs of increasing thickness. A good signal was retrieved with 1 W through 14 cm of tissue, which is an improvement from penetrating $3 - 5$ cm with 26 mW. If an OTPA is used in the diode-laser GAMAS-system then, based on the TiSa-laser measurements, light detection could be possible through larger geometries than what has so far been possible in GASMAS-settings.

By exploring different perspectives of GASMAS in large geometries, this project can be seen as a step on the way towards monitoring oxygen in adult lungs.

Outlook

As suggestion for future work within this field, the next step would be to improve the work of amplifying the diode-laser light with an OTPA. Benefits of increasing the tunable CW diode-laser power with an OTPA include 1) allowing light penetration into biologial tissue of larger geometries and 2) preserving the well-functioning WMS-techniques for signal-enhancement that have been proven successful for GASMAS lung measurements. In this project, a first simple OTPA-alignment method was used. The optical axis was defined with two irises, on which both the ASE of the OPTA and diode seed-laser was overlapped with the help of two mirrors. A lens with xyz-translation focussed the laser beam onto the OTPA crystal input. Probably, that the laser beam is aligned ideally and with high power on the 3 μm OTPA input aperture is critical for the amplification to work optimally. Developing better possibilities of adjusting the translation and angle of the OTPA in relation to the incident seed-laser could prove very beneficial. Hopefully, the proposed future work to incorporate an OTPA into the now-functioning GASMAS-system could help make GASMAS in large geometries possible.

Bibliography

1. Svanberg S. Gas in Scattering Media Absorption Spectroscopy. Encyclopedia of Analytical Chemistry 2019. DOI: `https://doi.org/10.1002/9780470027318.a9325.pub2`
2. Lewander M, Guan Z, Persson L, Olsson A and Svanberg S. Gas Analysis in Food Packages Using Tunable Diode Laser Spectroscopy. Optical Society of America 2008. DOI: `https://doi.org/10.1364/AOE.2008.SuR3`
3. Lundin P, Cocola L, Lewander M, Olsson A and Svanberg S. Non-intrusive head-space gas measurements by laser spectroscopy – Performance validation by a reference sensor. Journal of Food Engineering 2012; 11:612–7. DOI: `http://dx.doi.org/10.1016/j.jfoodeng.2012.03.008`
4. Svensson T, Andersson M, Rippe L, Svanberg S, Andersson-Engels S, Johansson J and Folestad S. VCSEL-based oxygen spectroscopy for structural analysis of pharmaceutical solids. Applied Physics 2008; 90:345–54. DOI: `https://doi.org/10.1007/s00340-007-2901-6`
5. Lewander M, Bruzelius A, Svanberg S, Svanberg K and Fellman V. Nonintrusive gas monitoring in neonatal lungs using diode laser spectroscopy: feasibility study. Journal of Biomedical Optics 2011; 16:127002-1 –127002-6. DOI: `https://doi.org/10.1117/1.3663211`
6. Krite Svanberg E, Lundin P, Larsson M, Åkeson J, Svanberg K, Svanberg S, Andersson-Engels S and Fellman V. Diode laser spectroscopy for noninvasive monitoring of oxygen in the lungs of newborn infants. Pediatric Research 2016; 79:621–8. DOI: `http://www.nature.com/doifinder/10.1038/pr.2015.267`
7. Krite Svanberg E, Larsson J, Rasmussen M, Larsson M, Leander D, Bergsten S, Bood J, Greisen G and Fellman V. Changes in pulmonary oxygen content are detectable with laser absorption spectroscopy: proof of concept in newborn piglets. Pediatric Research 2021; 89:823–9. DOI: `https://doi.org/10.1038/s41390-020-0971-x`
8. Lin Y, Lundin P, Krite Svanberg E, Svanberg K, Svanberg S and Sahlberg AL. Gas in Scattering Media Absorption Spectroscopy on Small and Large Scales: Towards the Extension of Lung Spectroscopic Monitoring to Adults. Translational Biophotonics 2021; 3. DOI: `https://doi.org/10.1002/tbio.202100003`
9. Boudoux C. Fundamentals of Biomedical Optics. Blurb, 2016
10. Svanberg S. Atomic and Molecular Spectroscopy. Springer, 2001
11. Demtröder W. Atoms, Molecules and Photons. Springer, 2018
12. Supplee J, Whittaker E and Lenth W. Theoretical description of frequency modulation and wavelength modulation spectroscopy. Applied Optics 1994. DOI: `https://doi.org/10.1364/ao.33.006294`
13. Reid J and Labrie D. Second-Harmonic Detection with Tunable Diode Lasers - Comparison of Experiment and Theory. Applied Physics 1981. DOI: `https://doi.org/10.1007/BF00692448`

14. Persson L, Andersson F, Andersson M and Svanberg S. Approach to optical inter-ference fringes reduction in diode laser absorption spectroscopy. Applied Physics 2007; 87:523–30. DOI: https://doi.org/10.1007/s00340-007-2593-y

15. Gordon Iea. The HITRAN 2020 molecular spectroscopic database. Journal of Quant-itative Spectroscopy and Radiative Transfer 2020; 277. DOI: https://doi.org/10.1016/j.jqsrt.2021.107949

16. Optical Amplifiers. Available from: https://www.thorlabs.com/newgrouppage9.cfm?objectgroup_id=14304 [Accessed on: 2022 Jun 8]

17. Lewander M. Laser Absorption Spectroscopy of Gas in Scattering Media. PhD thesis. Lund University, 2010

18. Alignment of a DFB MOPA System with DFB TPA Configuration. Available from: https://www.toptica-eagleyard.com/fileadmin/downloads/documents/eyP_AppNote_TPA_2-0.pdf [Accessed on: 2022 Jun 8]

19. Saleh BEA and Teich MC. Fundamentals of Photonics. Wiley, 2019

20. EYP-TPA-0765-01500-3006-CMT03-0000. 0.91. [Datasheet]. GmbH eagleyard Photon-ics. Rudower Chaussee 29 12489 Berlin GERMANY, 2017 Nov. Available from: https://www.toptica-eagleyard.com/fileadmin/downloads/data_sheets/EYP-TPA-0765-01500-3006-CMT03-0000.pdf

Appendix A

Table 1: Signal-to-noise ratio (SNR) of measurements with a continuous-wave (CW) diode-laser system used for oxygen GAs in Scattering Media Absorption Spectroscopy (GASMAS), on samples of boar lung and styrofoam. The samples contained ambient air or nitrogen gas. The number of samples (n), means and standard deviations (std) are indicated.

Continous Wave Measurements			
Sample	Gas	SNR	Mean (std)
Styrofoam (n = 1)	Air (n = 1)	17.664	NA
Lung (n = 29)	Air (n = 25)	3.6737	4.9589 (1.7712)
		4.2811	
		7.5603	
		6.7396	
		6.862	
		9.5757	
		2.6555	
		4.2774	
		2.5754	
		2.513	
		6.2798	
		6.0142	
		6.3264	
		4.2907	
		4.3848	
		4.3241	
		4.0865	
		4.9316	
		4.2436	
		4.5857	
		3.9565	
	Nitrogen (n = 4)	2.1425	2.0989 (0.3142)
		1.6826	
		2.4456	
		2.125	

Appendix B

Table 2: Power (mW) measured of light collected with a prism at the output-facet of an optical tapered amplifier (OTPA). The powers for the background, with only the seed-laser switched on, only the OTPA on and finally both laser and OPTA on are presented.

Laser output power (mW)	Output-power behind OTPA (mW)			
	Background	Laser	OTPA	Background, Laser and OTPA
14.5	0.29	0.28	0.44	0.55
37.7	0	0.31	0.51	0.55
50	0.19	0.19	0.58	2.3